NASA TECHNICAL NOTE

NASA TN D-5094

C.1

0131793

TECH LIBRARY KAFB, NM

NASA TN D-5094

LOAN COPY: RETURN TO
AFWL (WLIL-2)
KIRTLAND AFB, N MEX

DYNAMIC ANALYSIS OF PERMANENT MAGNET STEPPING MOTORS

by David J. Robinson

Lewis Research Center

Cleveland, Ohio

NATIONAL AERONAUTICS AND SPACE ADMINISTRATION • WASHINGTON, D. C. • MARCH 1969

TECH LIBRARY KAFB, NM
0131793

DYNAMIC ANALYSIS OF PERMANENT MAGNET STEPPING MOTORS

By David J. Robinson

Lewis Research Center
Cleveland, Ohio

NATIONAL AERONAUTICS AND SPACE ADMINISTRATION

For sale by the Clearinghouse for Federal Scientific and Technical Information
Springfield, Virginia 22151 – CFSTI price $3.00

ABSTRACT

A dynamic analysis of permanent magnet stepping motors for multistep operation is described. Linearized transfer functions for single-step responses are developed. Multistep operation, when the motor is driven by a current source, is analyzed by using phase plane techniques. Failure of the motor to operate for fixed stepping rates and load torques is discussed. Dimensionless curves showing maximum stepping rate as a function of motor parameters and load torque are developed and experimentally verified. The curves allowed the maximum stepping rate of a motor with viscous, inertial, and torque loads to be predicted from simple measurements of the motor parameters.

DYNAMIC ANALYSIS OF PERMANENT MAGNET STEPPING MOTORS

by David J. Robinson

Lewis Research Center

SUMMARY

Permanent magnet stepping motors are being applied as digital actuators. Analytical models of stepping motors have been developed that analyze the dynamic response to a single step. They have not, however, been expanded to analyze stepping motor performance during multistep operation.

An analytical study is presented herein that examines stepping motor performance during both single-step and multistep operation. A linearized single-step model is developed which allows the stepping motor to be defined in terms of a natural frequency and a damping ratio. A nonlinear analysis is also developed which, when a constant current source is assumed, allows the stepping motor to be analyzed for fixed stepping rates and applied load torques. It was found that the permanent magnet stepping motor cannot respond to a step command when the applied load torque becomes greater than 0.707 of the motor's stall torque. Also the motor cannot follow a sequential set of step commands if, during the sequence, the rotor lags the command position by more than two steps.

Based on these results, we developed and experimentally checked a set of dimensionless curves which express maximum normalized stepping rate as a function of normalized damping and normalized load torque. These curves allow the maximum stepping rate of a motor with viscous, inertial, and torque loads to be predicted from simple measurements of the motor parameters.

INTRODUCTION

In recent years, the use of digital control has found increased application in the field of automatic control systems. One inherent problem in applying digital control is in selected suitable digital actuators. One promising actuator is the permanent magnet (PM) stepping motor.

The application of stepping motors is not new. Proctor (ref. 1) reports that stepping motors were first used in servomechanisms in the early 1930's. During the development

of closed-loop servomechanisms in the World War II years, proportional analog activators largely replaced stepping motors in actuator applications. With the space age and the development of automatic digital systems, problems arose in using analog closed-loop servomechanisms because of the need for digital-to-analog (D/A) conversion techniques. This problem was particularly important in space applications because of the extra weight required for the D/A equipment.

The stepping motor has found increased applications as a digital actuator because it does not require D/A conversion. Nicklas (ref. 2) utilized a stepping motor as an actuator in a spacecraft instrumentation system. Giles and Marcus (ref. 3) reported on the use of stepping motors as control drum actuators for the SNAP-8 program.

To increase the application of the stepping motor, much analytical work has been done. Bailey (ref. 4) compares stepping motors with conventional closed-loop positioning systems. The stepping motor was modeled, for a single-step response, as a second-order linear approximation. O'Donohue (ref. 5) and Kieburtz (ref. 6) have developed similar mathematical models. These particular second-order models cannot be extended to adequately describe the dynamics of the stepping motor for multistep inputs. Bailey analyzed multistep inputs on a limited basis, by assuming that the time between application of the step command was long compared with the settling time of the response to each step input.

The work described in this report was conducted to develop analytical techniques to investigate multistep operation. The analysis is restricted to permanent magnet stepping motors; however, the techniques can be extended to other forms of stepping motors, electrical, pneumatic, or mechanical. Stepping motor operation is analyzed to determine an expression for developed torque. A linearized single-step analysis is presented to express motor performance in terms of a natural frequency and damping ratio. Phase plane techniques are used to extend the analysis to handle multistep commands supplied from a constant current source. From the analysis, a dimensionless curve is developed that allows the maximum stepping rate of a motor with viscous, inertial, and torque loads to be predicted from simple measurements of the motor parameters.

Simple experimental results from two stepping motors are presented. These results are used to check the analytical analysis.

DESCRIPTION OF PERMANENT MAGNET STEPPING MOTOR OPERATION

The permanent magnet (PM) stepping motor is an incremental device that accepts discrete input commands, and responds to these commands by rotating an output shaft in equal angular increments, called steps; one step for each input command. The angular position of the output shaft is controlled by the initial location and the number of input commands received. The angular velocity of the output shaft is controlled by the rate at which the input commands are carried out.

Simplified Permanent Magnet Stepping Motor

A simplified PM stepping motor is shown in figure 1. The PM stepping motor consists of a stator containing two or more phases wound on salient poles and a permanent magnet rotor of high permeability. When a stator winding is energized, a magnetic flux is set up which interacts with the permanent magnet rotor. The rotor will move in such a manner that the magnetic moment of the permanent magnet will aline with the field set up by the stator winding current. In referring to figure 1, assume winding 1 is energized such that a magnetic flux is set up with a direction from the face of salient pole 1 and into the face of salient pole 3. The rotor will aline as shown. If winding 2 is energized such that a magnetic field is set up with a direction from the face of salient pole 2 and into the face of salient pole 4, the rotor will turn such that the south magnetic pole of the rotor alines with salient pole face 2. If winding 1 is energized in the manner previously described, the rotor will move so that the south magnetic pole is again alined with salient pole face 1. However, if the current is reversed in winding 1 such that the magnetic field direction is from salient pole 3 and into salient pole 1; the rotor will move such that the south magnetic pole alines with salient pole 3 instead of salient pole 1. Thus, the position of the rotor of a PM stepping motor can be determined by a discrete set of stator winding excitations and a discrete set of current reversals in the stator windings.

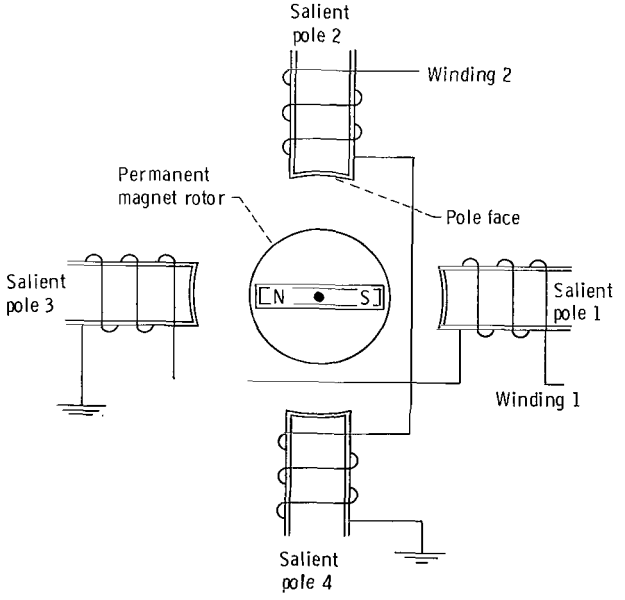

Figure 1. - Typical representation of permanent magnet stepping motor.

Synchronous Inductor Motor

There are several different PM stepping motor configurations available commercially. The most common types are derived from two- or four-phase ac synchronous motors. The synchronous inductor motor is one of these types and has received considerable attention in the literature for stepping motor applications (refs. 1 and 6 to 9).

As an aid in developing some general results, the torque developed by the synchronous inductor motor is examined. Figure 2(a) shows a simplified cross section of a two-phase synchronous inductor motor with four salient poles and five rotor teeth. The rotor tooth pitch is 72°, while the salient poles are located every 90°. One step corresponds to one-fourth of the rotor tooth pitch, or a rotor movement of 18°. One complete revolution of the rotor corresponds to 20 steps. Figure 2(b) shows an expanded layout of the rotor and stator. The expanded layout is used to simplify the graphical representation of the developed torque as the rotor moves relative to the stator salient poles.

Stepping the rotor is accomplished by reversing the direction of the current in one phase while holding the other phase constant. For a two-phase, four-salient-pole motor, the salient poles can form four possible magnetic pole combinations:

(1) Salient poles P_{1A} and P_{2A} are north magnetic poles, and salient poles P_{1B} and P_{2B} are south magnetic poles.

(2) Salient poles P_{1B} and P_{2A} are north magnetic poles, and salient poles P_{1A} and P_{2B} are south magnetic poles.

(3) Salient poles P_{1B} and P_{2B} are north magnetic poles, and salient poles P_{1A} and P_{2A} are south magnetic poles.

(4) Salient poles P_{1A} and P_{2B} are north magnetic poles, and salient poles P_{1B} and P_{2A} are south magnetic poles.

Figure 3(a) shows the developed torque as a function of rotor position for combination (1). The resultant curve is the summation of the torque curves due to the individual phases and, as will be discussed later, is assumed to be sinusodal. The equilibrium points of the resultant curve lie midway between the equilibrium points of the individual phases. Figure 3(b) shows the developed torque as a function of rotor position for combination (2). The equilibrium points of the resultant curve remain midway between the equilibrium points of the individual phases. Comparing the resultant curves of figures 3(a) and (b) show that the equilibrium points have shifted by 1/4 rotor tooth pitch. In like manner, figures 3(c) and (d) show the developed torque for combinations (3) and (4). If the motor is stepped by sequentially repeating the magnetic pole combinations, the rotor equilibrium points will be shifted by 1/4 rotor tooth pitch for each combination applied.

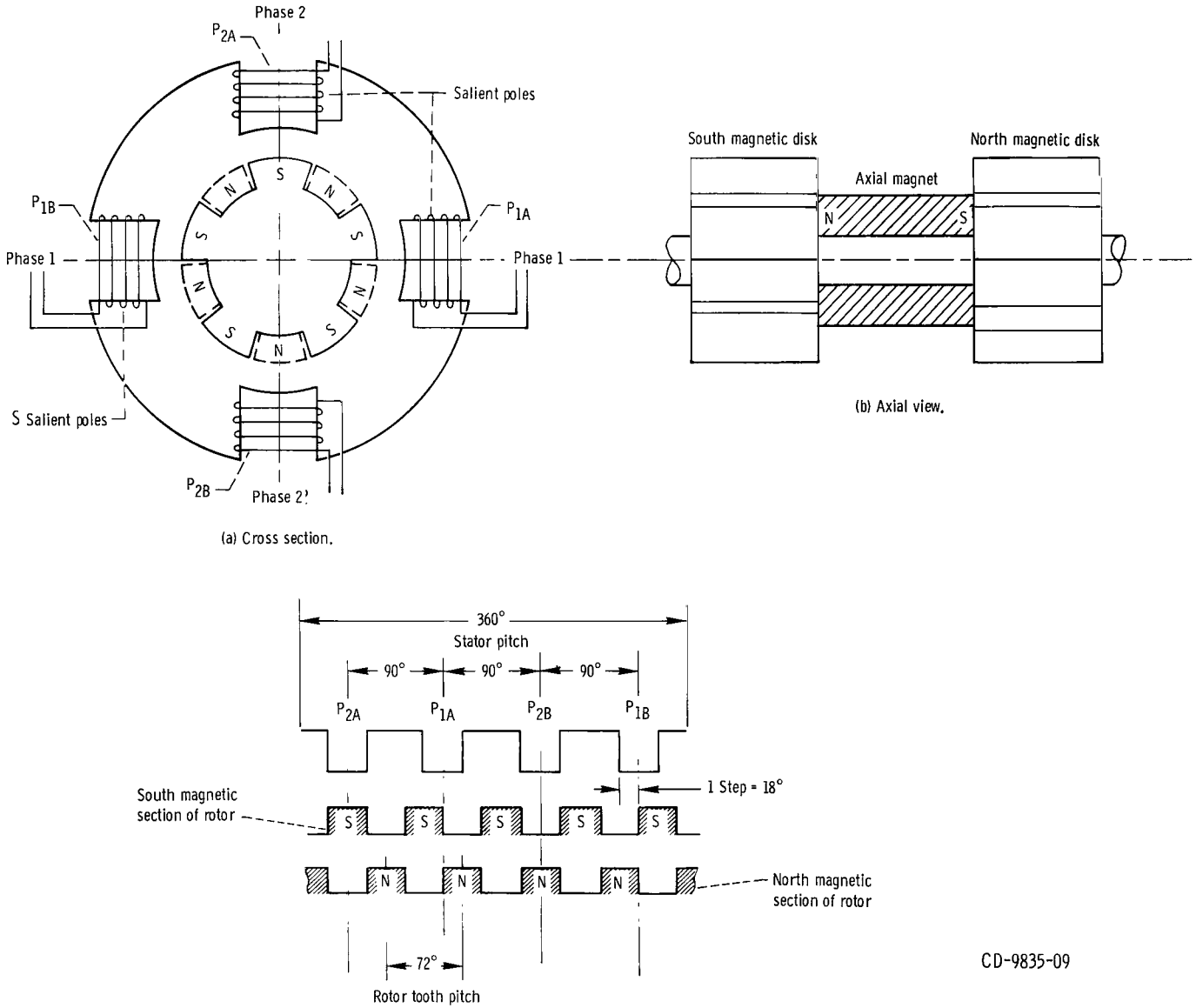

(a) Cross section.

(b) Axial view.

(c) Expanded rotor-stator layout.

Figure 2. - Simplified synchronous inductor motor.

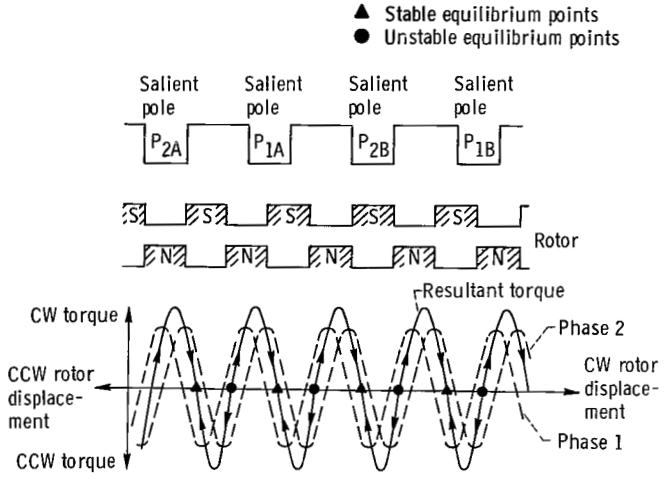

(a) Stator currents I_1 and I_2: salient poles P_{1A} and P_{2A} are north magnetic poles; P_{1B} and P_{2B} are south magnetic poles.

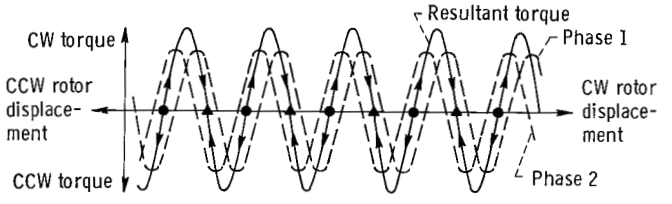

(b) Stator currents $-I_1$ and I_2: salient poles P_{1B} and P_{2A} are north magnetic poles; P_{1A} and P_{2B} are south magnetic poles.

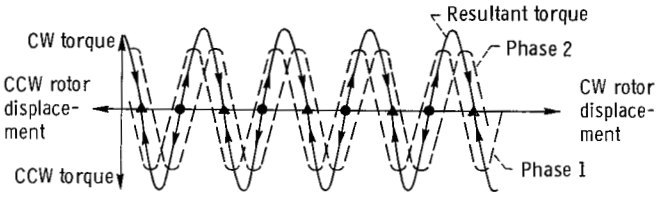

(c) Stator currents $-I_1$ and $-I_2$: salient poles P_{1B} and P_{2B} are north magnetic poles; P_{1A} and P_{2A} are south magnetic poles.

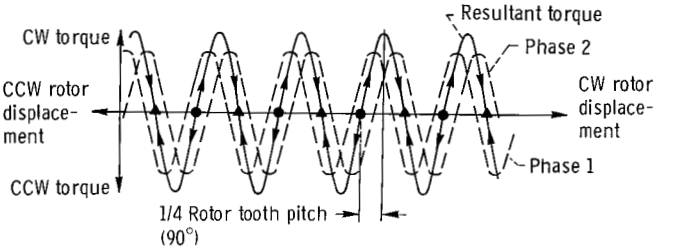

(d) Stator currents I_1 and $-I_2$: salient poles P_{1A} and P_{2B} are north magnetic poles; P_{1B} and P_{2A} are south magnetic poles.

Figure 3. - Torque as function of rotor position - both phases energized. Arrows indicate direction of developed torque about equilibrium points.

Analytical Development of Stepping Motor Torque

Torque is produced on the rotor of the PM stepping motor as the result of an interaction between the flux created by the stator windings and the permanent magnet rotor. In the PM stepping motor, the stator windings are wound in coils surrounding each salient pole. Assume that an energized stator winding produces a parallel magnetic field of density $\vec{B}$. Also assume that the rotor of the PM stepping motor is a thin bar magnet. The torque relations of a thin bar magnet in a parallel magnetic field are shown in figure 4.

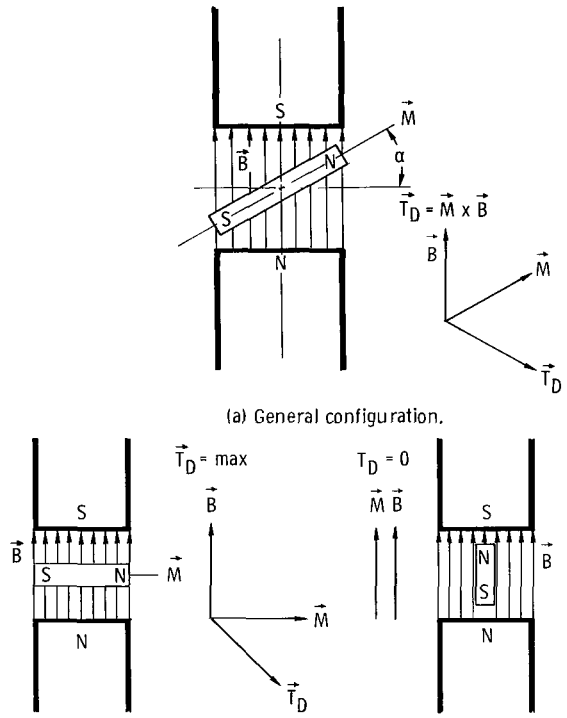

(a) General configuration.

(b) Maximum and minimum torque developed.

Figure 4. - Torque relations of thin-bar magnet in parallel magnetic field.

The bar magnet tends to turn in a direction such that its magnetic moment vector $\vec{M}$ will line up with the parallel magnetic field. The torque developed $\vec{T}_D$ is the cross product of the magnetic moment vector $\vec{M}$ and the magnetic flux density $\vec{B}$:

$$T_D = \vec{M} \times \vec{B} \tag{1}$$

(All symbols are defined in appendix A.) When figure 4(a) is used, the developed torque becomes

$$|\vec{T}_D| = |\vec{M}| \ |\vec{B}| \cos \alpha \tag{2}$$

Figure 4(b) shows that the maximum torque is developed when the permanent magnet is perpendicular to the parallel field. When the permanent magnet is parallel with the magnetic field, no torque is developed.

The magnetic moment of the thin bar magnet is proportional to the pole strength m and to the length l of the bar magnet. Thus,

$$|\vec{M}| = K_m l m \tag{3}$$

If the parallel magnetic field is produced by an ideal solenoid of n turns, the magnetic density is proportional to the number of turns and to the magnitude of the current I(t) flowing through the solenoid turns.

$$|\vec{B}| = K_I n I(t) \tag{4}$$

Thus, the torque developed on a thin bar magnet in a parallel magnetic field is given by.

$$T_D = K_I K_m l m n I(t) \cos \alpha \tag{5}$$

or

$$T_D = K_T I(t) \cos \alpha \tag{6}$$

where

$$K_T = K_m l m n K_I$$

Since the maximum torque developed occurs when $\alpha = 0$,

$$T_{max} = K_T I(t) \tag{7}$$

Thus, the developed torque can be expressed by

$$T_D = T_{max} \cos \alpha \tag{8}$$

Equation (8) may not be an exact model when applied to the PM stepping motor, since the stator windings are not ideal solenoids and the rotor is not a bar magnet. The magnetic flux set up by the stator windings has a distribution effect across the surface of the salient pole face. Similarly, the rotor has distributional effects due to its configuration.

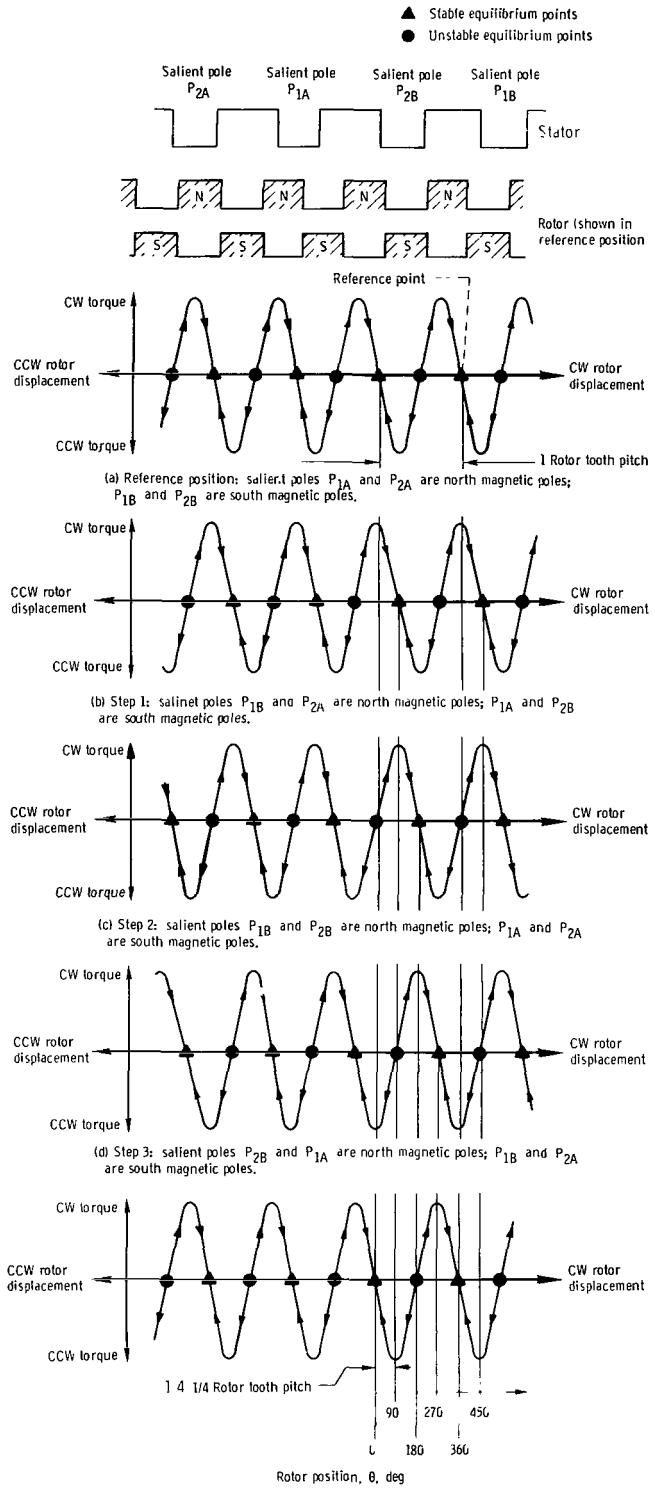

(a) Reference position: salient poles P_{1A} and P_{2A} are north magnetic poles; P_{1B} and P_{2B} are south magnetic poles.

(b) Step 1: salinet poles P_{1B} and P_{2A} are north magnetic poles; P_{1A} and P_{2B} are south magnetic poles.

(c) Step 2: salient poles P_{1B} and P_{2B} are north magnetic poles; P_{1A} and P_{2A} are south magnetic poles.

(d) Step 3: salient poles P_{2B} and P_{1A} are north magnetic poles; P_{1B} and P_{2A} are south magnetic poles.

(e) Step 4: salient poles P_{1A} and P_{2A} are north magnetic poles; P_{1B} and P_{2B} are south magnetic poles.

Figure 5. - Resultant torque as function of rotor position for four-step sequence. Arrows indicate direction of developed torque about equilibrium points.

In addition, the magnitude of the torque depends upon the number of phases energized, since the magnetic structure of the motor will be used more efficiently when all the phases are energized.

For a given stepping motor, each rotor movement of 1/4 tooth pitch corresponds to an angular rotation φ in mechanical degrees. Define an angle θ such that, when the rotor moves 1/4 tooth pitch, θ varies by 90°. The angle θ is related to the mechanical angle of rotation φ taken during each step by the number of teeth on the rotor.

$$\theta = N_{RT}\varphi \tag{9}$$

The resultant developed stepping motor torque from each step command can be generalized by assuming that the developed torque varies sinusoidally when the rotor moves 1/4 tooth pitch. By superimposing the torque produced by each pole pair, the developed torque can be expressed by

$$T_D = T_{max} \sin \theta \tag{10}$$

Figure 5 shows the resultant curves for developed torque as a function of position for a four-step sequence in a synchronous inductor motor. In figure 5(a), equilibrium point X is an arbitrary reference point. As the rotor is moved, the resultant developed torque is given by

$$T_D = -T_{max} \sin \theta \tag{11}$$

Figure 5(b) shows the resultant torque curve for the first step command. The torque is given by

$$T_D = -T_{max} \sin(\theta - 90^{\circ}) \tag{12}$$

$$T_D = T_{max} \cos \theta \tag{13}$$

Figure 5(c) shows the resultant torque curve for the second step command. The torque is given by

$$T_D = -T_{max} \sin(\theta - 180^{\circ}) \tag{14}$$

$$T_D = T_{max} \sin \theta \tag{15}$$

Figure 5(d) shows the resultant torque curve for the third step command. The torque is given by

$$T_D = -T_{max} \sin(\theta - 270^o) \tag{16}$$

$$T_D = -T_{max} \cos \theta \tag{17}$$

Figure 5(e) shows the resultant torque curve for the fourth step command. The torque is given by

$$T_D = -T_{max} \sin(\theta - 360^o) \tag{18}$$

$$T_D = -T_{max} \sin \theta \tag{19}$$

This is the same result as for the reference point, equation (11). Thus, the torque developed in a PM stepping motor for any step command sequence can be given by a combination of the four equations:

$$T_D = -T_{max} \sin \theta \tag{20}$$

$$T_D = T_{max} \cos \theta \tag{21}$$

$$T_D = T_{max} \sin \theta \tag{22}$$

$$T_D = -T_{max} \cos \theta \tag{23}$$

Equation (7) stated that the maximum torque developed per phase was related to the stator current by

$$T_{max} = K_T I(t) \tag{24}$$

If the time between steps is long compared with the rise time for the stator current, the equation for T_{max} can be written

$$T_{max} = K_T I_1 = K_T I_2 = K_T I \tag{25}$$

The developed torque for one phase becomes

$$T_D = K_T I \sin \theta \tag{26}$$

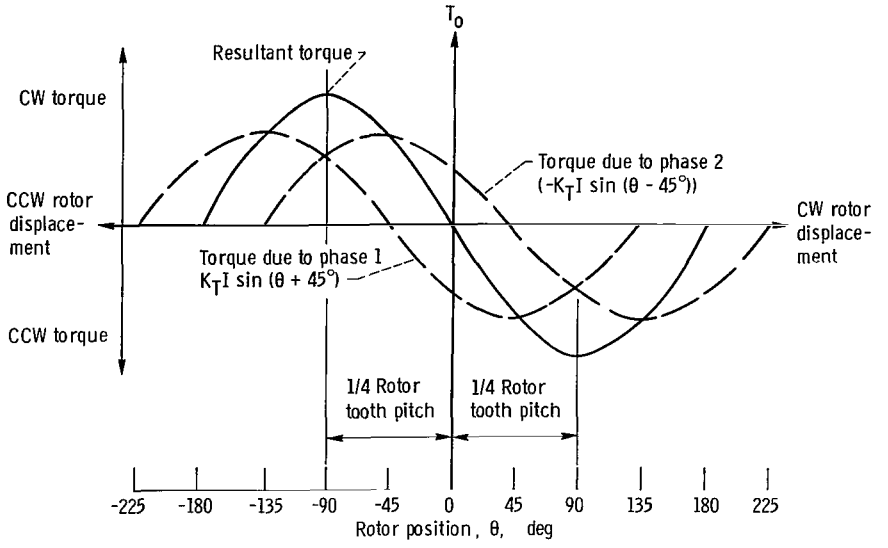

Figure 6. - Torque as function of rotor position for generalized permanent magnet stepping motor - both phases energized.

With the aid of figure 6, equation (26) can be extended to include the case when both phases are energized and the magnitudes of the stator currents are assumed to be equal:

$$T_D = \left[-K_T I \sin(\theta - 45^o)\right] + \left[-K_T I \sin(\theta + 45^o)\right] \tag{27}$$

$$T_D = -K_T I\left[\sin(\theta - 45^o) + \sin(\theta + 45^o)\right] \tag{28}$$

$$T_D = -\sqrt{2}\, K_T I \sin\theta \tag{29}$$

The minus sign in equation (29) is due to the reference point chosen. It indicates that for a clockwise (CW) θ, the developed torque will move the rotor in a counterclockwise (CCW) direction.

PM Stepping Motor Single-Step Analysis

A schematic representation of the PM stepping motor is shown in figure 7. The voltages supplied to the stator windings are given by

$$E_1(t) = RI_1(t) + L\frac{dI_1(t)}{dt} + E_v \tag{30}$$

$$E_2(t) = RI_2(t) + L\frac{dI_2(t)}{dt} + E_v \tag{31}$$

The induced voltage E_v generated in the stator is due to the magnetic rotor moving relative to the stator magnetic poles.

It is assumed that the rotor velocity vector remains perpendicular to the stator flux during the entire step. However, due to the geometry of the stator, the magnitude of the stator flux density is distributed in the stator. When this distribution is assumed to be sinusoidal and Maxwell's equations are used, the induced voltage can be given by

$$E_v = \frac{K_v}{N_{RT}}\frac{d\theta(t)}{dt}\sin\theta(t) \tag{32}$$

Thus, the differential equation for the stator voltage per winding becomes

$$E_1(t) = RI_1(t) + L\frac{dI_1(t)}{dt} + K_v\frac{d\theta(t)}{dt}\sin\theta(t) \tag{33}$$

$$E_2(t) = RI_2(t) + L\frac{dI_2(t)}{dt} + K_v\frac{d\theta(t)}{dt}\cos\theta(t) \tag{34}$$

In responding to a step command, the developed torque produced by the motor must overcome the mechanical load placed on the rotor. The mechanical load includes

(1) The inertial torque $J\left[d^2\varphi(t)/dt^2\right]$, which includes the inertia of the motor and the inertia of any load imposed on the stepping motor shaft

(2) The viscous damping torque $D\left[d\varphi(t)/dt\right]$, which includes the motor damping and any viscous damping on the motor shaft

(3) Torque due to Coulomb friction $T_f\left\{\left[d\varphi(t)/dt\right]\Big/\left[\left|d\varphi(t)/dt\right|\right]\right\}$ (Coulomb friction is defined as a friction independent of the magnitude of the relative velocity of the surfaces in contact, but dependent on the direction of the relative velocity.)

(4) External load torque applied to the motor shaft $T_L(t)$

In referring to figure 7, the equation of motion of the PM stepping motor can be expressed by

$$\begin{aligned} T_D &= K_T I_2(t)\cos\theta(t) - K_T I_1(t)\sin\theta(t) \\ &= \frac{J}{N_{RT}}\frac{d^2\theta(t)}{dt^2} + \frac{D}{N_{RT}}\frac{d\theta(t)}{dt} + T_f\frac{\dfrac{d\theta(t)}{dt}}{\left|\dfrac{d\theta(t)}{dt}\right|} + T_L(t) \end{aligned} \tag{35}$$

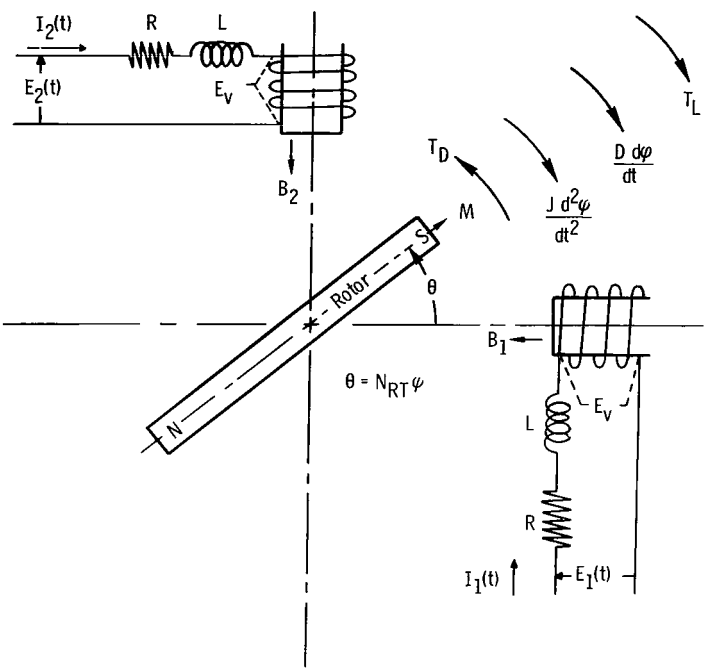

Figure 7. - Schematic representation of permanent magnet stepping motor for a single step.

Linearized Model

Equations (33) to (35) are nonlinear differential equations because of the torque-producing term in each of the equations. These equations can be linearized about an operating point by expanding them in a Taylor series (ref. 10) of the form

$$f_1(X_1, X_2) = f_1(X_{1,0}, X_{2,0}) + \frac{\partial f_1}{\partial X_1}(X_1, X_2)\Bigg|_{\substack{X_{1,0}\\X_{2,0}}}(X_1 - X_{1,0}) + \frac{\partial f_1}{\partial X_2}(X_1, X_2)\Bigg|_{\substack{X_{1,0}\\X_{2,0}}}(X_2 - X_{2,0}) + \ldots \tag{36}$$

Linearizing equations (33) to (36) results in

$$K_T I_2(t) \cos\theta(t) - K_T I_1(t) \sin\theta(t) = K_T I_{2,0} \cos\theta_0 - K_T I_{2,0} \sin\theta_0\, \Delta\theta(t) + K_T \cos\theta_0\, \Delta I_2(t) - K_T I_{1,0} \sin\theta_0 - K_T I_{1,0} \cos\theta_0\, \Delta\theta(t) - K_T \sin\theta_0\, \Delta I_1(t) \tag{37}$$

$$\frac{J}{N_{RT}}\frac{d^2\theta(t)}{dt^2}+\frac{D}{N_{RT}}\frac{d\theta(t)}{dt}+T_f\frac{\frac{d\theta(t)}{dt}}{\left|\frac{d\theta(t)}{dt}\right|}+T_L(t)=\frac{J}{N_{RT}}\left\{\left(\frac{d^2\theta}{dt^2}\right)_0+\Delta\left[\frac{d^2\theta(t)}{dt^2}\right]\right\}$$

$$+\frac{D}{N_{RT}}\left\{\left(\frac{d\theta}{dt}\right)_0+\Delta\left[\frac{d\theta(t)}{dt}\right]\right\}$$

$$+T_f\frac{\left(\frac{d\theta}{dt}\right)_0}{\left|\left(\frac{d\theta}{dt}\right)_0\right|}+T_{L,0}+\Delta T_L(t) \qquad (38)$$

$$E_{2,0}+\Delta E_2(t)=R\left[I_{2,0}+\Delta I_2(t)\right]+L\left\{\left(\frac{dI_2}{dt}\right)_0+\Delta\left[\frac{dI_2(t)}{dt}\right]\right\}+\frac{K_v}{N_{RT}}\left(\frac{d\theta}{dt}\right)_0\cos\theta_0$$

$$+\frac{K_v}{N_{RT}}\cos\theta_0\,\Delta\left[\frac{d\theta(t)}{dt}\right]-\frac{K_v}{N_{RT}}\left(\frac{d\theta}{dt}\right)_0\sin\theta_0\,\Delta\theta(t) \qquad (39)$$

$$E_{1,0}+\Delta E_1(t)=R\left[I_{1,0}+\Delta I_1(t)\right]+L\left\{\left(\frac{dI_1}{dt}\right)_0+\Delta\left[\frac{dI_1(\theta)}{dt}\right]\right\}+\frac{K_v}{N_{RT}}\left(\frac{d\theta}{dt}\right)_0\sin\theta_0$$

$$+\frac{K_v}{N_{RT}}\sin\theta_0\,\Delta\left(\frac{d\theta}{dt}\right)+\frac{K_v}{N_{RT}}\left(\frac{d\theta}{dt}\right)_0\cos\theta_0\,\Delta\theta(t) \qquad (40)$$

Transfer Function About an Operating Point at Beginning of a Step

The linearized equations are first considered about an operating point at the beginning of a step. The constraining equation neglecting friction becomes

$$K_T I_{2,0}\cos\theta_0-K_T I_{1,0}\sin\theta_0=\frac{J}{N_{RT}}\left(\frac{d^2\theta}{dt^2}\right)_0+\frac{D}{N_{RT}}\left(\frac{d\theta}{dt}\right)_0+T_{L,0} \qquad (41)$$

Now assume that the voltage applied to winding 1 is held constant and the motor is stepped by energizing winding 2. Assume the initial conditions

$$\left(\frac{d\theta}{dt}\right)_0 = \left(\frac{d^2\theta}{dt^2}\right)_0 = I_{2,0} = 0$$

Also, since the voltage applied to winding 1 is being held constant, $\Delta E_1(t) = 0$. From the differential equation at the operating point

$$-K_T I_{1,0} \sin \theta_0 = T_{L,0} \tag{42}$$

Equation (42) establishes θ_0 at the beginning of the step

$$\theta_0 = \sin^{-1} \frac{T_{L,0}}{-K_T I_{1,0}} \tag{43}$$

For an excursion about the operating point, equations (37) and (38) can be combined as follows:

$$K_T \cos \theta_0 \, \Delta I_2(t) - K_T I_{1,0} \cos \theta_0 \, \Delta\theta(t) - K_T \sin \theta_0 \, \Delta I_1(t) = \frac{J}{N_{RT}} \Delta\left[\frac{d^2\theta(t)}{dt^2}\right] + \frac{D}{N_{RT}} \times \Delta\left[\frac{d\theta(t)}{dt}\right] + \Delta T_L(t) \tag{44}$$

Making use of the identities

$$\sin \theta_0 = -\frac{T_{L,0}}{K_T I_{1,0}} \tag{45}$$

$$\cos \theta_0 = \frac{\sqrt{K_T^2 I_{1,0}^2 - T_{L,0}^2}}{K_T I_{1,0}} \tag{46}$$

equation (44) can be written

$$\frac{J}{N_{RT}}\Delta\left[\frac{d^2\theta(t)}{dt^2}\right]+\frac{D}{N_{RT}}\Delta\left(\frac{d\theta}{dt}\right)+\left(\sqrt{K_T^2I_{1,0}^2-T_{L,0}^2}\right)\Delta\theta(t)=\frac{K_T\sqrt{K_T^2I_{1,0}^2-T_{L,0}^2}}{K_TI_{1,0}}\Delta I_2(t)$$

$$+\frac{T_{L,0}}{I_{1,0}}\Delta I_1(t)-\Delta T_L(t) \qquad (47)$$

Also, equations (39) and (40), for an excursion about the operating point, can be written as

$$\Delta E_2(t)=R\Delta I_2(t)+L\,\Delta\left[\frac{dI_2(t)}{dt}\right]+\frac{K_v}{N_{RT}}\,\frac{\sqrt{K_T^2I_{1,0}^2T_{L,0}^2}}{K_TI_{1,0}}\,\Delta\left[\frac{d\theta(t)}{dt}\right] \qquad (48)$$

$$0=R\Delta I_1(t)+L\,\Delta\left[\frac{dI_1(t)}{dt}\right]-\frac{K_vT_{L,0}}{N_{RT}K_TI_{1,0}}\,\Delta\left[\frac{d\theta(t)}{dt}\right] \qquad (49)$$

A transfer function relating rotor position, stator voltage, and load torque can be derived by taking the Laplace transforms of equations (47) to (49). The derivations of the Laplace transformations are found in appendix B. The resultant linearized transfer function about an operating point at the beginning of a step is as follows:

$$\Delta\theta(S)=\frac{K_T\sqrt{1-\frac{T_{L,0}^2}{K_T^2I_{1,0}^2}}\left[\Delta E_2(S)+\frac{E_{2,0}}{S}\right]-(R+LS)\,\Delta T_L(S)}{JLS^3+(DL+JR)S^2+\left(DR+\frac{K_TK_v}{N_{RT}}+LK_TI_{1,0}\sqrt{1-\frac{T_{L,0}^2}{K_T^2I_{1,0}^2}}\right)S+RK_TI_{1,0}\sqrt{1-\frac{T_{L,0}^2}{K_T^2I_{1,0}^2}}} \qquad (50)$$

If the initial load torque $T_{L,0}$ is 0, equation (50) can be reduced to

$$\Delta\theta(S)=\frac{K_T\left[\Delta E_2(S)+\frac{E_{2,0}}{S}\right]-(R+LS)\,\Delta T_L(S)}{JLS^3+(DL+JR)S^2+\left(DR+\frac{K_TK_v}{N_{RT}}+LK_TI_{1,0}\right)S+RK_TI_{1,0}} \qquad (51)$$

Equations (50) and (51) show that the resultant linearized transfer function about an operating point at the beginning of a step results in a third-order system. The resultant linearized transfer function can be used to examine the effect of an initial value of load torque on the step response. It can also be used to examine the effects of inductance, generated back electromotive force (emf), inertia, and damping on the step response. However, the choice of an operating point at the beginning of a step makes experimental verification of the resulting model difficult.

Transfer Functions About an Operating Point at End of a Step

Consider the transfer function of the PM stepping motor about an operating point when the motor is in equilibrium at the end of a step with both phases energized. This operating point is chosen because the resulting transfer function can be easily verified experimentally. At the end of the step, the initial conditions are $\left[(d\theta)/(dt)\right]_0 = \left[(d^2\theta)/(dt^2)\right]_0 = 0$ and $I_{1,0} = I_{2,0} = I$. For an excursion about the operating point the constraining equation at the operating point is

$$K_T I_{2,0} \cos \theta_0 - K_T I_{1,0} \sin \theta_0 = T_{L,0} \tag{52}$$

or

$$\cos \theta_0 - \sin \theta_0 = \frac{T_{L,0}}{K_T I} \tag{53}$$

Equation (53) establishes θ_0. If $T_{L,0} = 0$, then $\theta_0 = 45^\circ$. The linearized equations about the operating point equating friction are

$$-K_T I\left[\sin \theta_0 + \cos \theta_0\right] \Delta\theta(t) + K_T \cos \theta_0 \, \Delta I_2(t) - K_T \sin \theta_0 \, \Delta I_1(t)$$

$$= \frac{J}{N_{RT}} \Delta\left[\frac{d^2\theta(t)}{dt^2}\right] + \frac{D}{N_{RT}} \Delta\left[\frac{d\theta(t)}{dt}\right] + \Delta T_L(t) \tag{54}$$

$$\Delta E_2(t) = R \, \Delta I_2(t) + L \, \Delta\left[\frac{dI_2(t)}{dt}\right] + \frac{K_v}{N_{RT}} \cos \theta_0 \, \Delta\left[\frac{d\theta(t)}{dt}\right] \tag{55}$$

$$\Delta E_1(t) = R\,\Delta I_1(t) + L\,\Delta\left[\frac{dI_1(t)}{dt}\right] + \frac{K_v}{N_{RT}}\sin\theta_0\,\Delta\left[\frac{d\theta(t)}{dt}\right] \tag{56}$$

The Laplace transformations of equations (54) to (56) are

$$\Delta\theta(S) = \frac{K_T\cos\theta_0\,\Delta I_2(S) - K_T\sin\theta_0\,\Delta I_1(S) - \Delta T_L(S)}{\frac{JS^2}{N_{RT}} + \frac{DS}{N_{RT}} + K_T I\left[\sin\theta_0 + \cos\theta_0\right]} \tag{57}$$

$$\Delta I_2(S) = \frac{\Delta E_2(S) + \frac{E_{2,0}}{S} - \frac{K_v}{N_{RT}}\cos\theta_0 S\,\Delta\theta(S)}{R + LS} \tag{58}$$

$$\Delta I_1(S) = \frac{\Delta E_1(S) + \frac{E_{1,0}}{S} - \frac{K_v}{N_{RT}}\sin\theta_0 S\,\Delta\theta(S)}{R + LS} \tag{59}$$

Combining equations (57) to (59) gives the resultant linearized equation for both phases energized about an operating point at the end of a step

$$\Delta\theta(S) = \frac{\frac{K_T\cos\theta_0}{R+LS}\left[\Delta E_2(S) + \frac{E_{2,0}}{S}\right] - \frac{K_T\sin\theta_0}{R+LS}\left[\Delta E_1(S) + \frac{E_{1,0}}{S}\right] - \Delta T_L(S)}{\frac{JS^2}{N_{RT}} + \frac{DS}{N_{RT}} + \frac{K_T K_v}{N_{RT}(R+LS)}\left(\cos^2\theta_0 - \sin^2\theta_0\right)S + K_T I\left(\sin\theta_0 + \cos\theta_0\right)} \tag{60}$$

For no initial load torque ($T_{L,0} = 0$), the constraining equation (eq. (53)) yields $\theta_0 = 45^\circ$. Thus,

$$\Delta\theta(S) = \frac{\frac{0.707K_T}{R+LS}\left[\Delta E_2(S) + \frac{E_{2,0}}{S}\right] - \frac{0.707K_T}{R+LS}\left[\Delta E_1(S) + \frac{E_{1,0}}{S}\right] - \Delta T_L(S)}{\frac{JS^2}{N_{RT}} + \frac{DS}{N_{RT}} + \sqrt{2}\,K_T I} \tag{61}$$

For load torque disturbances about the operating point at the end of the step and the initial load torque equal to 0, the transfer function is a second-order system

$$\theta(S) = \frac{-\frac{1}{J}\Delta T_L(S)(N_{RT})}{S^2 + \frac{D}{JS} + \frac{\sqrt{2K_T I N_{RT}}}{J}} \tag{62}$$

This result is important for two reasons. First, it allows the stepping motor to be described in terms of a natural frequency and damping ratio. Second, these parameters can easily be determined experimentally.

Equation (62) has been developed in terms of θ, such that one step equals 90^o. Equation (62) can be written in terms of the actual mechanical degrees for a particular stepping motor. Since

$$\frac{d^2\varphi(t)}{dt^2} + \frac{D}{J}\frac{d\varphi(t)}{dt} + \frac{\sqrt{2}\,K_T I}{J}\,\theta(t) = -\frac{\Delta T_L(t)}{J} \tag{63}$$

it follows that

$$\Delta\varphi(S) = -\frac{\frac{1}{J}\Delta T_L(S)}{S^2 + \frac{D}{JS} + \frac{N_{RT}\sqrt{2}\,K_T I}{J}} \tag{64}$$

The natural frequency obtained from equation (64) is given by

$$\omega_N = \sqrt{\frac{N_{RT}\sqrt{2}\,K_T I}{J}} \tag{65}$$

The natural frequency of the PM stepping motor is increased by

(1) Decreasing the inertia

(2) Increasing the number of rotor teeth

(3) Increasing the magnitude of the stator current

The upper bound on the natural frequency due to inertia is often limited by the load inertia. However, minimizing the rotor inertia increases the natural frequency when the load

inertia is not the limiting factor. The natural frequency of the stepping motor can also be expressed in terms of the stall torque T_S with both phases energized

$$T_S = \sqrt{2}\, K_T I \tag{66}$$

Thus,

$$\omega_N = \sqrt{\frac{N_{RT} T_S}{J}} \tag{67}$$

The damping ratio of equation (64) is given by

$$2\zeta\omega_N = \frac{D}{J} \tag{68}$$

$$\zeta = \frac{D}{2\sqrt{JN_{RT}T_S}} \tag{69}$$

The damping ratio is increased by increasing the viscous damping, or by decreasing the inertia. The damping ratio is decreased by increasing the number of rotor teeth or by increasing the maximum torque by increasing the stator current.

The natural frequency and the damping ratio of the linearized model of the PM stepping motor can also be evaluated by considering a small change in $\Delta\theta$ from the equilibrium point. Consider the linearized equations about the point of stable equilibrium with the stator current held constant and no applied load torque. The linearized equations reduce to

$$-K_T I(\sin\theta_0 + \cos\theta_0)\,\Delta\theta(t) = \frac{J}{N_{RT}}\,\Delta\left[\frac{d^2\theta(t)}{dt^2}\right] + \frac{D}{N_{RT}}\,\Delta\left[\frac{d\theta(t)}{dt}\right] \tag{70}$$

The Laplace transform of equation (70) is

$$-K_T I(\sin\theta_0 + \cos\theta_0)\,\Delta\theta(S) = \frac{J}{N_{RT}}\left\{S^2\,\Delta\theta(S) - S\,\Delta\theta(0) - \left(\frac{d\theta}{dt}\right)_0 - \Delta\left[\frac{d\theta(0)}{dt}\right] - \frac{\left(\frac{d\theta}{dt}\right)_0}{S}\right\}$$

$$+\frac{D}{N_{RT}}\left[S\,\Delta\theta(S) - \Delta\theta(0) - \frac{\left(\frac{d\theta}{dt}\right)_0}{S}\right] \qquad (71)$$

For a small initial displacement $\Delta\theta(0)$ and initial conditions $\theta_0 = 45^\circ$ and $\Delta[d\theta(0)/dt] = (d\theta/dt)_0 = (d^2\theta/dt^2)_0 = 0$, equation (71) can be rewritten as

$$-N_{RT}\sqrt{2}\,K_T I\,\Delta\theta(S) = (JS^2 + DS)\,\Delta\theta(S) - (JS + D)\,\Delta\theta(0) \qquad (72)$$

where

$$\Delta\theta(S) = \frac{\left(S + \frac{D}{J}\right)\Delta\theta(0)}{S^2 + \frac{D}{JS} + \frac{\sqrt{2}\,K_T I N_{RT}}{J}} \qquad (73)$$

Equation (73) can be used to evaluate the natural frequency and the damping ratio of the linearized model about the stable equilibrium point.

PHASE PLANE ANALYSIS

The linearized mathematical model of the PM stepping motor was developed to analyze the single-step response of the PM stepping motor. For multistep operation, the response of the PM stepping motor for a given load torque is governed by

(1) The rate of the input pulses

(2) The current transients in the stator windings

(3) The mechanical parameters of the rotor

The linearized model cannot be used to analyze multistep responses because the model fails to account for motor failures caused by excessive input stepping command.

The transient response of the stator current has a significant effect on the stepping motor response as the stepping rate is increased. Even if the back emf induced in the stator is not significant, the current turnon transient affects the maximum torque developed by the motor. Consider the electrical (L/R) time constant of the stator windings. If the time between the application of step commands approaches this time, the current will not reach its expected value. The maximum torque developed by the motor is reduced, and thus, the natural frequency of the stepping motor is reduced. The amount of load torque which the motor can step against is also reduced.

In general, stepping motor drive circuits are designed to compensate for stator current transients. The drive circuit tends to act as a constant current source by controlling the stator current independently of the inductance or generated emf. A typical constant current drive source used to compensate a stepping motor is presented by Zeller (ref. 11).

For multistep analysis, it is assumed that a drive circuit is used which approximates a current source for stepping motors. The stator currents are assumed to be constant and to have magnitudes equal to I or -I during each step.

Analytical Model Assuming Constant Current Source

The assumption of a constant current source simplifies the analytical model of the PM stepping motor. It also permits the response of the motor to be studied for a series of input pulses. Because the current is independent of $dI(t)/dt$ and $d\theta(t)/dt$, the stator winding equations become

$$E_1 = \pm IR \tag{74}$$

$$E_2 = \pm IR \tag{75}$$

The sign in each equation is determined by the input pulse sequence.

The differential equation of rotor motion can be reduced to a second-order nonlinear differential equation. For the rotor at the equilibrium position, the developed motor torque has been shown to be

$$T_D = K_T I \sin\left[\theta(t) - 45^o\right] + K_T I \sin\left[\theta(t) + 45^o\right] \tag{76}$$

A step command requires that the rotor angle θ advance 90^o. The developed torque generated by the motor to accomplish this step is given by

$$T_D = K_T I \sin\left\{90^o - \left[\theta(t) - 45^o\right]\right\} + K_T I \sin\left\{90^o - \left[\theta(t) + 45^o\right]\right\} \tag{77}$$

or

$$T_D = K_T I \left\{\sin\left[135^o - \theta(t)\right] + \sin\left[45^o - \theta(t)\right]\right\} \tag{78}$$

Equation (78) reduces to

$$T_D = \sqrt{2}\, K_T I \cos\,\theta(t) \tag{79}$$

Equating equation (79) to the mechanical load of the motor results in

$$\sqrt{2}\, K_T I \cos\,\theta(t) = \frac{J}{N_{RT}} \frac{d^2\theta(t)}{dt^2} + \frac{D}{N_{RT}} \frac{d\theta(t)}{dt} + T_f \frac{\dfrac{d\theta(t)}{dt}}{\left|\dfrac{d\theta(t)}{dt}\right|} + T_L(t) \tag{80}$$

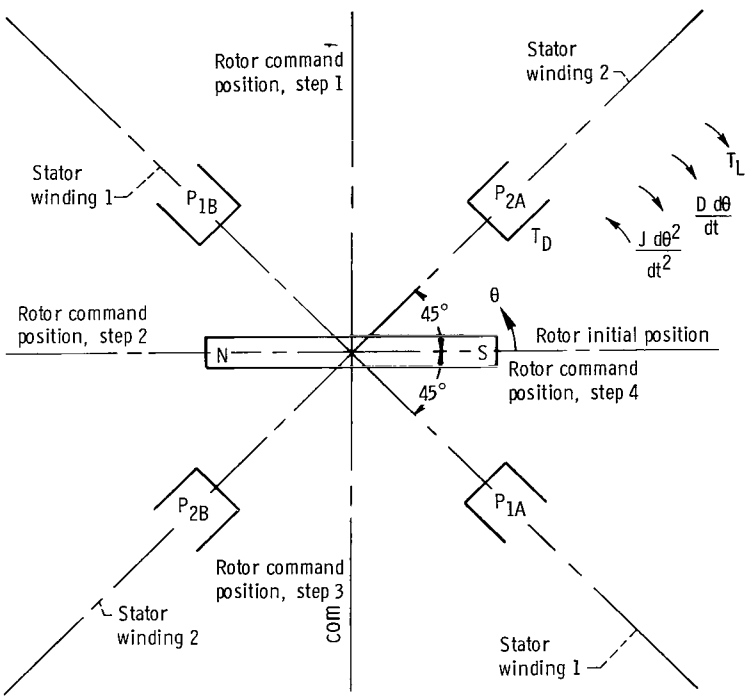

Figure 8. - Schematic representation of rotor command positions. Multistep operation.

Multistep Analysis Assuming Constant Current Source

Equation (80) can be extended to include multistep operation. Each step command calls for the rotor equilibrium position to shift by 90^{o}. Examine figure 8 and assume the rotor is initially at 0^{o}. The equations for the developed torque for a series of steps are then

Step 1: $$T_D = K_T I \sin\left\{90^{o} - \left[\theta(t) - 45^{o}\right]\right\} + K_T I \sin\left\{90^{o} - \left[\theta(t) + 45^{o}\right]\right\} \quad (81)$$

Step 2: $$T_D = K_T I \sin\left\{180^{o} - \left[\theta(t) - 45^{o}\right]\right\} + K_T I \sin\left\{180^{o} - \left[\theta(t) + 45^{o}\right]\right\} \quad (82)$$

Step 3: $$T_D = K_T I \sin\left\{270^{o} - \left[\theta(t) - 45^{o}\right]\right\} + K_T I \sin\left\{270^{o} - \left[\theta(t) + 45^{o}\right]\right\} \quad (83)$$

Step 4: $$T_D = K_T I \sin\left\{360^{o} - \left[\theta(t) - 45^{o}\right]\right\} + K_T I \sin\left\{360^{o} - \left[\theta(t) + 45^{o}\right]\right\} \quad (84)$$

Step 5: $$T_D = K_T I \sin\left\{450^{o} - \left[\theta(t) - 45^{o}\right]\right\} + K_T I \sin\left\{450^{o} - \left[\theta(t) + 45^{o}\right]\right\} \quad (85)$$

and so forth. These equations reduce to

Step 1: $$T_D = \sqrt{2}\, K_T I \cos\theta(t) \quad (86)$$

Step 2: $$T_D = \sqrt{2}\, K_T I \sin\theta(t) \quad (87)$$

Step 3: $$T_D = -\sqrt{2}\, K_T I \cos\theta(t) \quad (88)$$

Step 4: $$T_D = -\sqrt{2}\, K_T I \sin\theta(t) \quad (89)$$

Step 5: $$T_D = \sqrt{2}\, K_T I \cos\theta(t) \quad (90)$$

and so forth. The basic equation for multistep operation becomes

$$\sqrt{2}\,K_T I \sin\left[\theta_c - \theta(t)\right] = \frac{J}{N_{RT}}\frac{d^2\theta(t)}{dt^2} + \frac{D}{N_{RT}}\frac{d\theta(t)}{dt} + T_f \frac{\frac{d\theta(t)}{dt}}{\left|\frac{d\theta(t)}{dt}\right|} + T_L(t) \tag{91}$$

Normalized Model for Multistep Operation

The second-order nonlinear differential equation obtained in equation (91) lends itself to phase plane analysis. This equation can be considered as the transient solution to a set of initial conditions. By specifying the initial conditions $\theta(0)$ and $d\theta(0)/dt$, the solution for all positive time is completely determined. An advantage of the phase plane analysis is that trajectories representing the transient solution of the equation can be determined without solving the equation for the dependence of position on time.

Equation (91) can be normalized to reduce the number of parameters. By using the linearized analysis, the normalization can be performed to allow the use of experimental data. Dividing equation (91) by the stall torque $\left(T_S = \sqrt{2}\,K_T I\right)$ results in

$$\sin\left[\theta_c - \theta(t)\right] = \frac{J}{N_{RT}\sqrt{2}\,K_T I}\frac{d^2\theta(t)}{dt^2} + \frac{D}{N_{RT}\sqrt{2}\,K_T I}\frac{d\theta(t)}{dt} + \frac{T_f}{\sqrt{2}\,K_T I}\frac{\frac{d\theta(t)}{dt}}{\left|\frac{d\theta(t)}{dt}\right|} + \frac{T_L}{\sqrt{2}\,K_T I} \tag{92}$$

Recall that the natural frequency of the linearized second-order model is given by

$$\omega_N = \sqrt{\frac{N_{RT}\sqrt{2}\,K_T I}{J}} \tag{93}$$

Equation (92) can be simplified by defining a new time parameter in terms of the natural frequency:

$$\tau = \omega_N t \tag{94}$$

$$\frac{d}{d\tau} = \frac{1}{\omega_N}\frac{d}{dt} = \sqrt{\frac{J}{N_{RT}\sqrt{2}\,K_T I}}\frac{d}{dt} \tag{95}$$

$$\frac{d^2}{d\tau^2} = \frac{J}{N_{RT}\sqrt{2}\,K_T I}\frac{d^2}{dt^2} \tag{96}$$

$$\frac{D}{N_{RT}\sqrt{2}\,K_T I}\frac{d}{dt} = \frac{D}{\sqrt{N_{RT}\sqrt{2}\,K_T IJ}}\frac{d}{d\tau} = \bar{D}\frac{d}{d\tau} \tag{97}$$

Equation (97) can also be defined in terms of the damping ratio

$$\zeta = \frac{D}{2\omega_N J} = \frac{\sqrt{N_{RT}\sqrt{2}\,K_T IJ}}{2\sqrt{\frac{N_{RT}\sqrt{2}\,K_T I}{J}}}\left(\frac{\bar{D}}{J}\right) = \frac{\bar{D}}{2} \tag{98}$$

or

$$\bar{D} = 2\zeta \tag{99}$$

Also, normalizing the friction and load torques gives

$$\bar{T}_f = \frac{T_f}{\sqrt{2}\,K_T I} = \frac{T_f}{T_S} \tag{100}$$

and

$$\bar{T}_L = \frac{T_L}{\sqrt{2}\,K_T I} = \frac{T_L}{T_S} \tag{101}$$

Thus, equation (92) can be written with θ and θ_c specified in radians

$$\sin(\theta_c - \theta) = \frac{d^2\theta}{d\tau^2} + \bar{D}\frac{d\theta}{d\tau} + \bar{T}_f\frac{\frac{d\theta}{d\tau}}{\left|\frac{d\theta}{d\tau}\right|} + \bar{T}_L \tag{102}$$

Time can be eliminated from equation (102) by defining

$$\left.\begin{aligned} V &= \frac{d\theta}{d\tau} \\ \frac{dV}{d\tau} &= \frac{dV}{d\theta}\frac{d\theta}{d\tau} = V\frac{dV}{d\theta} \end{aligned}\right\} \tag{103}$$

Rewriting equation (103) in terms of position θ and velocity V results in

$$\sin(\theta_c - \theta) = V\frac{dV}{d\theta} + \overline{D}V + \overline{T}_f\frac{V}{|V|} + \overline{T}_L \tag{104}$$

The phase plane solution to equation (104) is a plot of velocity V as a function of position θ. The initial conditions $V(0)$ and $\theta(0)$ locate an initial point in the phase plane. The trajectory through this point describes the response of equation (104) for all positive time. The slope of the trajectory is given by

$$\frac{dV}{d\theta} = \frac{\sin(\theta_c - \theta) - \overline{D}V - \overline{T}_f\frac{V}{|V|} - \overline{T}_L}{V} \tag{105}$$

For a given motor with a specified value of friction, the slope of the trajectories is a function of three variables,

$$\frac{dV}{d\theta} = f\left(\theta, V, \overline{T}_L\right) \tag{106}$$

Thus, the unique response to a set of initial conditions must be specified in terms of the load torque, assuming that the motor is loaded by a speed independent torque of magnitude T_L. In the normalized equations, θ and θ_c must be specified in terms of radians.

Phase Plane Analysis by Delta Method

There are several graphical methods to determine the phase plane trajectories. For single-step analysis, the most convenient method is the delta method (ref. 10). The delta method assumes that the trajectories can be approximated by arcs of circles with origins on the θ-axis. In figure 9(a), δ gives the center of a circular arc through point P_1. Comparing similar triangles,

$$\frac{dV}{d\theta} = -\frac{\beta}{V} = -\frac{\theta + \delta}{V} \tag{107}$$

$$-\delta = \theta + V\frac{dV}{d\theta} \tag{108}$$

To determine a trajectory using equation (108), first select a point P_1 and solve for delta. The value of delta will determine the center of an arc r_c that will pass through point P_1. Notice that the center of the arc always lies on the θ-axis. After drawing a segment through point P_1, select a point P_2 on the segment. Compute a new delta and new arc center, etc. Figure 9(b) illustrates the method. Using equation (104) with

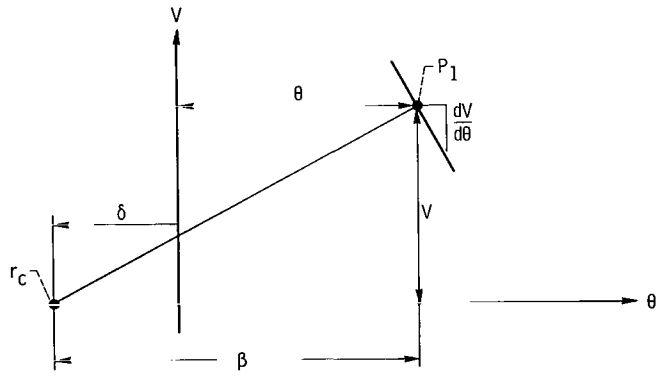

(a) Determination of center of circular arc through point P_1.

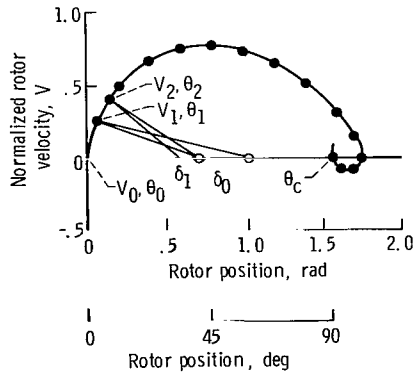

(b) Use of delta method.
V dV/dθ = cos(θ - V).

Figure 9. - Graphical solution of a phase plane trajectory by delta method.

$V(0) = \theta(0) = \overline{T}_f = T_L = 0$, $\theta_c = \pi/2$, and $\overline{D} = 1.0$ results in

$$\frac{V\,dV}{d\theta} = \cos\theta - V \tag{109}$$

$$-\delta = \theta + V\frac{dV}{d\theta} = \theta + \cos\theta - V \tag{110}$$

The process for computing the trajectory continues until the equilibrium point is reached.

Time can be computed along the trajectory (ref. 12). The relation between time, position, and velocity is given by

$$\tau = \int \frac{1}{V}\,d\theta \tag{111}$$

For a segment along the trajectory,

$$\tau_{N+1} - \tau_N = \frac{\theta}{V_{av}} \tag{112}$$

or

$$\tau_{N+1} - \tau_N = \frac{\theta_{N+1} - \theta_N}{\frac{1}{2}\left(V_{N+1} + V_N\right)} \tag{113}$$

The total time is the summation of the increments of time along the entire trajectory.

Single-step response. - For a single-step response the phase plane is useful in analyzing

(1) The transient response to a set of initial conditions

(2) The effect of load torque T_L on the transient response

(3) Other nonlinear effects, in particular Coulomb friction, provided they are built into the model

The equation for a single-step response was given in equation (104) as

$$\sin(\theta_c - \theta) = V\frac{dV}{d\theta} + \overline{D}V + \overline{T}_f\frac{V}{|V|} + \overline{T}_L \tag{114}$$

The step response will first be analyzed for $\overline{T}_f = \overline{T}_L = 0$. Equation (114) reduces to

$$\sin(\theta_c - \theta) = V \frac{dV}{d\theta} + \overline{D}V \tag{115}$$

Assume that the rotor is initially at rest and that the step command will move the rotor from 0^o to 90^o as shown in figure 8. The equation for the step becomes

$$\sin\left(\frac{\pi}{2} - \theta\right) = V \frac{dV}{d\theta} + \overline{D}V \tag{116}$$

or

$$\cos\ \theta = V \frac{dV}{d\theta} + \overline{D}V \tag{117}$$

For a given value of the normalized damping ratio $\overline{D}$, equation (117) describes a trajectory in the phase plane for a given set of initial conditions.

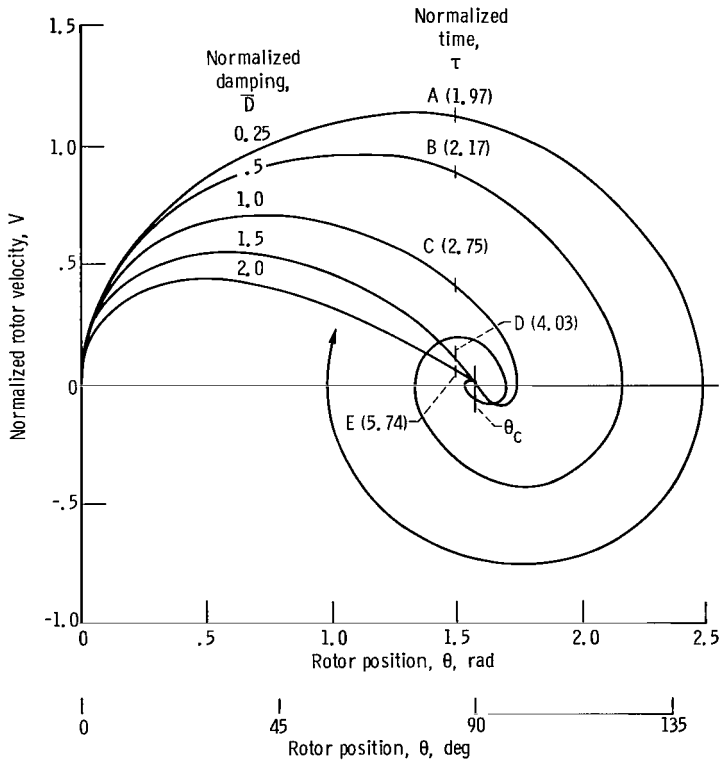

Figure 10. - Effect of normalized damping on single-step response. Normalized frictional torque $\overline{T}_f$, 0; rotor command position θ_c, 1.57 radians.

Figure 10 shows the effect of $\bar{D}$ on the step response. Increasing $\bar{D}$ makes the response less oscillatory and increases the rise time for each step response. In figure 10, the normalized time is given for each step response when θ reaches 1.50 radians or about 95 percent of the command value of 1.57 radians (90^{o}). The normalized time varies from 1.97 to 5.74 as $\bar{D}$ varies from 0.25 to 2.0.

Effect of load torque. - The addition of load torque causes an offset in the equilibrium position of the rotor. Load torque also slows down the step response. With load torque applied, the initial position of the rotor is determined by the equilibrium point of the previous step. Figure 11 illustrates this effect. Figure 11(a) shows the developed motor torque when $T_L = 0$. Assume the equilibrium position with no load torque before the step command is given is 0^{o}. The previous step command required to reach this position is given by

$$\sin(0^{o} - \theta) = V\frac{dV}{d\theta} + \bar{D}V \tag{118}$$

or

$$-\sin\theta = V\frac{dV}{d\theta} + \bar{D}V \tag{119}$$

The equilibrium position is given by

$$\left.\begin{aligned} -\sin\theta &= 0 \\ \text{or} \qquad & \\ \theta &= 0^{o}(0 \text{ radians}) \end{aligned}\right\} \tag{120}$$

These form the initial conditions for the next step. Notice that at this position no motor torque is developed. If the rotor is moved about this point, the motor develops a torque which tends to drive it back to the point of equilibrium. When the next step is commanded, maximum motor torque is applied to the rotor for acceleration. As the rotor moves toward 90^{o}, the amount of available torque is reduced until the 90^{o} position is reached. At this point, the developed torque is again 0.

Figure 11(b) shows the developed motor torque for a normalized load torque of 0.4. For the previous step, the equilibrium position has shifted 23.6^{o}. This shift is due to the fact that some motor torque is required to hold the load torque. The initial equilibrium position of -23.6^{o} was determined from

$$-\sin\theta = V\frac{dV}{d\theta} + \bar{D}V + 0.4 \tag{121}$$

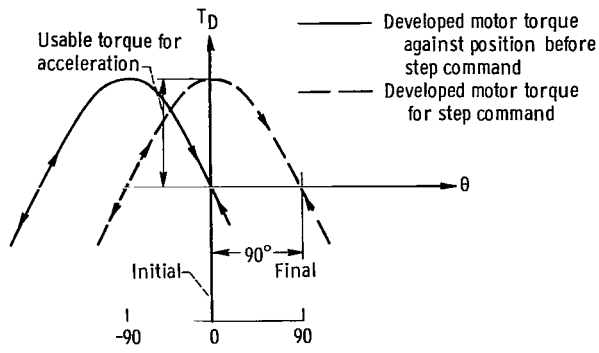

(a) $\overline{T}_L = 0.$

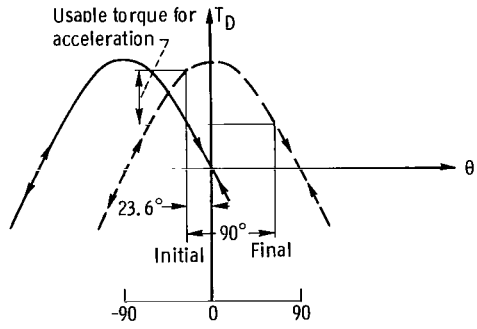

(b) $\overline{T}_L = 0.4.$

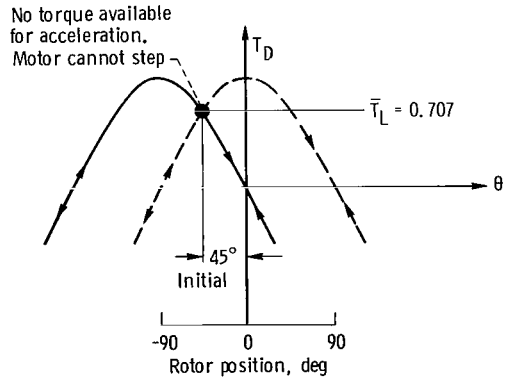

(c) $\overline{T}_L = 0.707.$

Figure 11. - Effect of normalized load torque $\overline{T}_L$ on developed motor torque for a step command. Arrows indicate direction in which developed motor torque acts.

When the rotor reaches equilibrium,

$$\left.\begin{aligned} -\sin\theta &= 0.4 \\ \theta &= -23.6^{\circ}(0.645 \text{ radians}) \end{aligned}\right\} \tag{122}$$

The shifted equilibrium position reduces the amount of motor torque that is available to accelerate the rotor to the next step. The torque that is available for acceleration is given by

$$\cos\theta - \overline{T}_L = V\frac{dV}{d\theta} + \overline{D}V \tag{123}$$

The amount of motor torque available for acceleration decreases with increasing load torque until $\overline{T}_L = 0.707$. From figure 11(c) for a load torque of 0.707, the rotor position offset is 45°. When the next step is commanded,

$$\cos\left(\frac{\pi}{4} - 0.707\right) = V\frac{dV}{d\theta} + \overline{D}V \tag{124}$$

$$0 = V\frac{dV}{d\theta} + \overline{D}V \tag{125}$$

there is no motor torque available to accelerate the rotor, and a step command cannot be accomplished. The motor can statically hold a load torque equal in value to the stall torque of the motor. But the motor cannot step a load torque that is equal to or greater than 0.707 of the motor's stall torque T_S. Thus, a normalized load torque of 0.707 will cause the PM stepping motor to fail to respond to a step command.

Figure 12 shows the step response in the phase plane for various values of load torque. Normalized damping $\overline{D}$ is given as 1.0. Notice that although the initial and final rotor positions are offset by the load torque, the distance between these positions is 90° (1.57 radians). Thus, load torque does not alter the size of the step, just the initial and final positions of the rotor.

Figure 12 illustrates the effect of load torque on the speed of response. The maximum velocity reached is reduced with increasing load torque. This is a direct result of the available motor torque to accelerate the rotor. Notice that with increasing load torque the amount of position overshoot is reduced. Also shown in figure 12 is the normalized time for the rotor to move 50 percent of its step. The time is increased with increasing load torque.

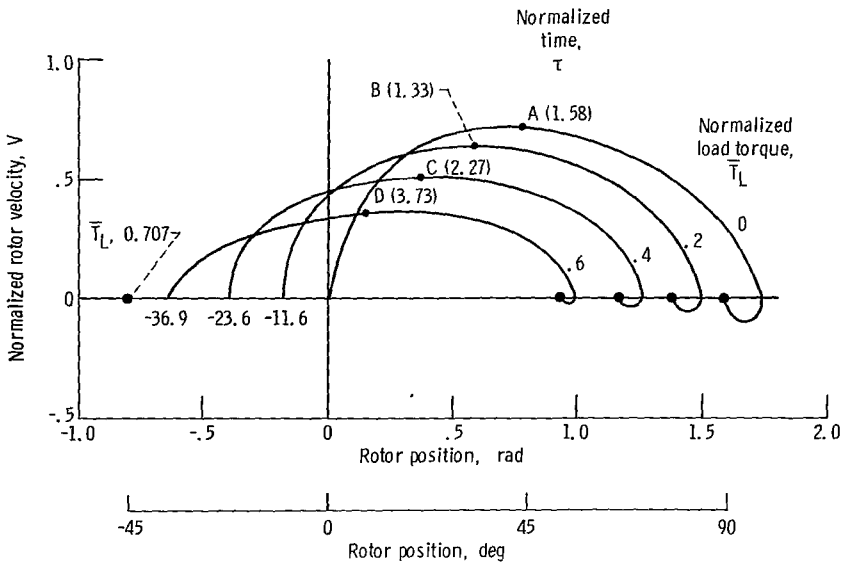

Figure 12. - Effect of normalized load torque on single-step response. Normalized damping, 1.0; frictional torque, 0.

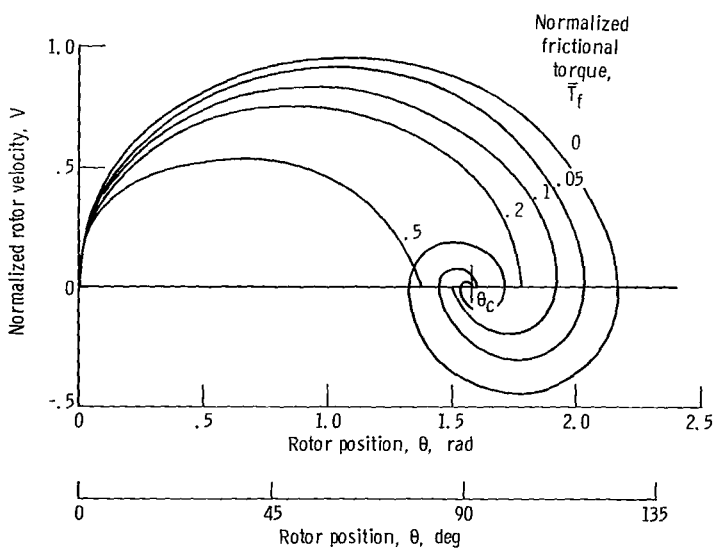

Figure 13. - Effect of normalized Coulomb friction on single-step response without load torque. Normalized damping, 0.5; normalized load torque, 0.

Effect of Coulomb friction. - Coulomb friction changes a given step size. Figure 13 illustrates the step response for various values of T_f with $T_L = 0$ and $D = 0.5$. Near the command position, the developed motor torque becomes small. If $T_f > \cos \theta$ when $V = 0$, the friction will hold the rotor, causing an offset from the command position. Thus, the equilibrium position lies in a band about the command position. The size of the band is determined by the amount of friction present. The speed of response is also reduced by friction. The reduction is small, however, unless a large amount of friction is present.

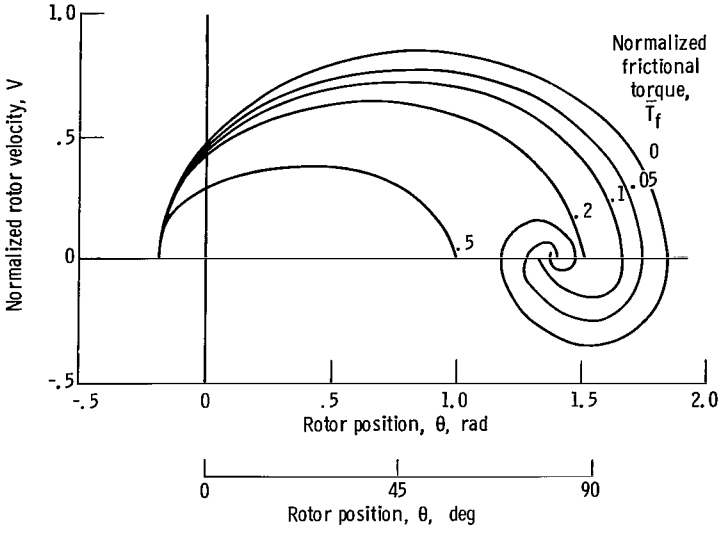

Figure 14. - Effect of normalized Coulomb friction on single-step response with load torque. Normalized damping, 0.2; normalized load torque, 0.5.

Combined effects. - Figure 14 illustrates the effect of friction combined with load torque. The effects are similar to those experienced with load torque alone. The final rotor position for a given step is determined by the values of load torque and friction present. The effect of T_f on stepping motor operation will not be considered further in this report since the frictional torque magnitude is generally small and its effects are somewhat similar to the load torque effects.

Multistep analysis. - The real advantage of using the phase plane in analyzing the stepping motor is that the analysis can be extended to include multistep operation. In multistep operation, each input step to the motor commands the rotor to move to a new position 90^o away from the existing command position. The dynamic equation that relates the motor movement is equation (104). If the time between the application of input steps is long, the rotor may reach the new point of equilibrium before the next step command is applied. As the rate of step commands is increased, the rotor may not reach the new equilibrium point. At the instant the next step command is applied, the position

and velocity of the rotor form initial conditions for the new equation of rotor motion. The step commands are applicable to unidirectional or bidirectional rotor movements.

The phase plane for multistep analysis can be considered as a series of trajectories for each possible dynamic equation given by the step commands. Time is computed along the trajectories and is used to indicate the time for the application of the next step command. As an illustration, consider the following series of input commands with $\overline{T}_f = 0$:

Step 1:
$$\sin\left(\frac{\pi}{2} - \theta\right) = \cos\theta = V\frac{dV}{d\theta} + \overline{D}V + T_L \tag{126}$$

Step 2:
$$\sin(\pi - \theta) = \sin\theta = V\frac{dV}{d\theta} + \overline{D}V + T_L \tag{127}$$

Step 3:
$$\sin\left(\frac{3\pi}{2} - \theta\right) = -\cos\theta = V\frac{dV}{d\theta} + \overline{D}V + \overline{T}_L \tag{128}$$

Step 4:
$$\sin(2\pi - \theta) = -\sin\theta = V\frac{dV}{d\theta} + \overline{D}V + \overline{T}_L \tag{129}$$

Step 5:
$$\sin\left(\frac{5\pi}{2} - \theta\right) = \cos\theta = V\frac{dV}{d\theta} + \overline{D}V + \overline{T}_L \tag{130}$$

Figure 15 shows a phase plane portrait for this series of steps. The trajectory is for $D = 0.25$ and $\overline{T}_L = 0$. Consider a normalized stepping period of $\Delta\tau = 1.31$.

The step commands are applied at the following normalized times:

Step 1: $\tau = 0,\ \theta_c = 90^\circ\left(\frac{\pi}{2}\text{ radians}\right)$

Step 2: $\tau = 1.31,\ \theta_c = 180^\circ\ (\pi\text{ radians})$

Step 3: $\tau = 2.62,\ \theta_c = 270^\circ\left(\frac{3\pi}{2}\text{ radians}\right)$

Step 4: $\tau = 3.93,\ \theta_c = 360^\circ\ (2\pi\text{ radians})$

Step 5: $\tau = 5.24,\ \theta_c = 450^\circ\left(\frac{5\pi}{2}\text{ radians}\right)$

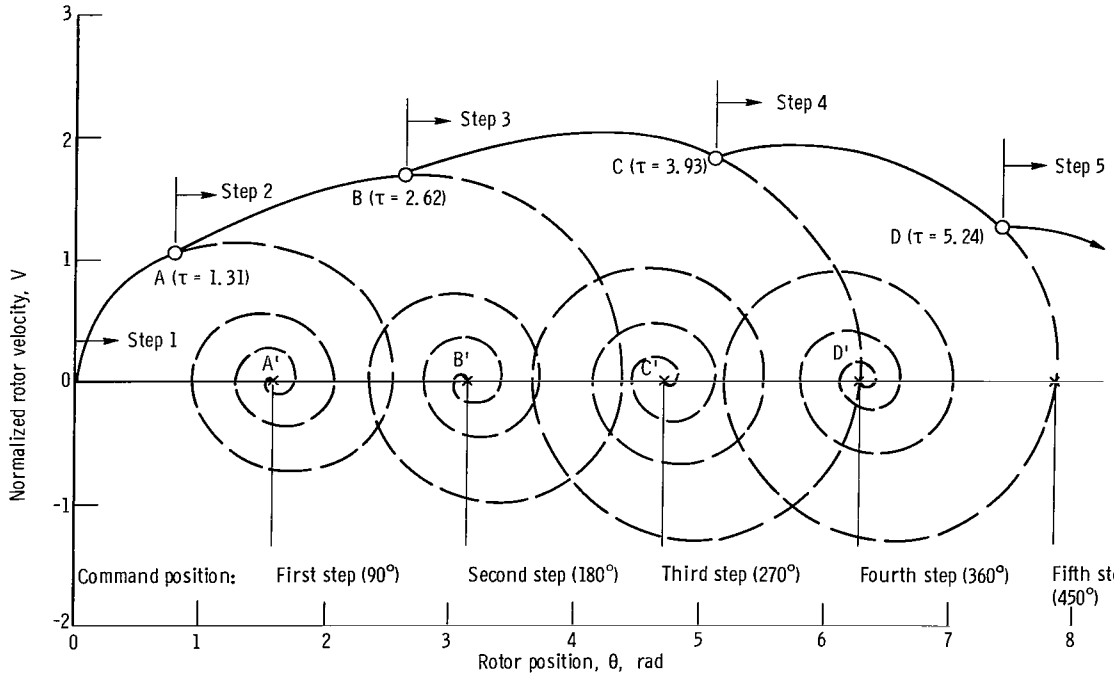

Figure 15. - Phase plane portrait for multistep input with no load torque.

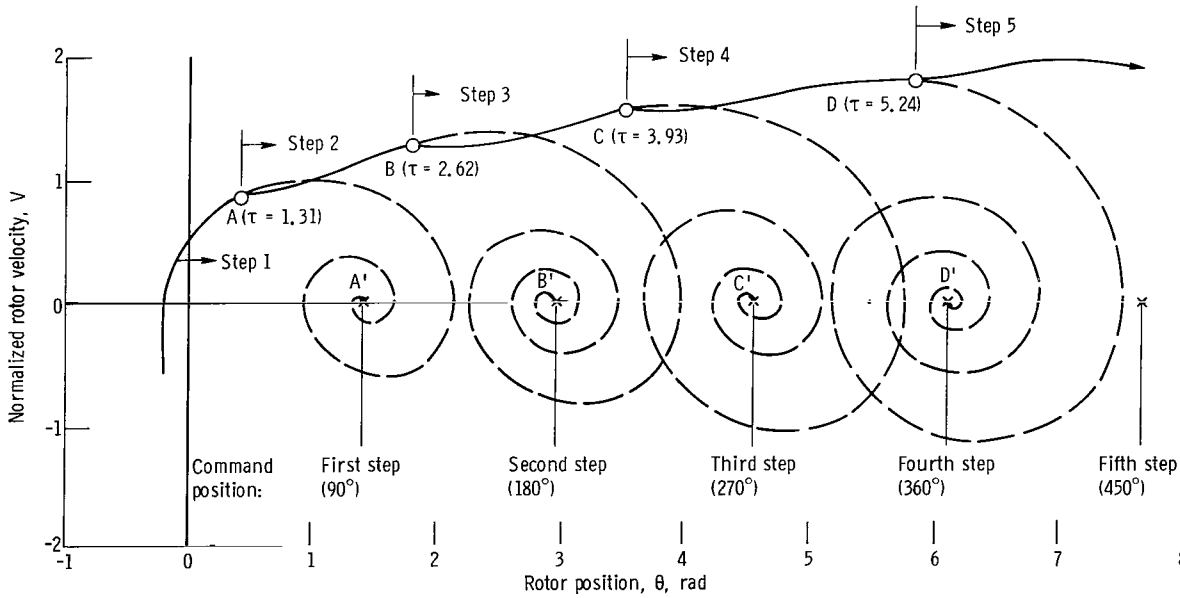

Figure 16. - Phase plane portrait for multistep input with normalized load torque equal to 0.2.

The initial conditions for step 1 are $V(0) = \theta(0) = 0$. The trajectory is governed by equation (126) and is shown in figure 15 between $\theta = 0$, $V = 0$, and point A. At point A, the total response time τ is 1.31, and step 2 is applied. The values of V and θ at point A become the initial conditions for the response of step 2. The equation governing step 2 is equation (127). The trajectory moves from point A to point B. At point B, the total time τ is 2.62. The third step command is applied and is governed by equation (128). The values of V and θ at point B become the initial conditions for equation (129). This process is continued for each step applied. The rate of stepping can be changed by simply changing the time between steps $\Delta\tau$.

The dashed trajectories in figure 15 show the phase plane trajectories if the succeeding commands are not applied. Curve 0A' is for a single-step command, 0B' is for a two-step command, and so forth. The response is oscillatory in each case, but each trajectory reaches its correct command position. The oscillations of the trajectories as they approach the equilibrium position are a function of the maximum velocity reached during the stepping sequence.

Figure 16 is a phase plane portrait of the same stepping sequence but with a load torque $\overline{T}_L$ of 0.2. The addition of load torque causes the rotor velocity to build up at a slower rate than in the case of no load torque. Without load torque, the rotor velocity peaks during the third step. With the load torque, the velocity does not peak until the fifth step. The dashed trajectories in figure 16 show the phase plane trajectories if the succeeding commands are not applied. A comparison of these trajectories clearly shows the applied load torque slows down the speed of response.

Phase Plane Analysis by Method of Isoclines

The phase portrait for the differential equation of the PM stepping motor can be used to determine whether the stepping motor will fail for a given stepping rate with a given value of load torque. The delta method provides a convenient way of constructing the phase trajectories for a given set of initial conditions and lends itself to computer solution. However, the entire family of phase trajectories can be graphically examined by developing the phase portrait using the method of isoclines (ref. 12). This method develops the phase plane by plotting curves, called isoclines, of constant trajectory slope.

The slope of the stepping motor differential equation is given by

$$\frac{dV}{d\theta} = \frac{\sin(\theta_c - \theta) - \overline{T}_L}{V} - \overline{D} \tag{131}$$

The slope of the differential equation must be specified in terms of a given $\overline{D}$ and $\overline{T}_L$.

The value of $\overline{D}$ is determined by the specific system in which it is applied. For the following analysis, $\overline{D}$ is chosen as 0.25. The load torque will be neglected in the following analysis. For a step command of 90^{o}, the slope is given by

$$\frac{dV}{d\theta} = \frac{\cos \theta}{V} - 0.25 \tag{132}$$

Figure 17 shows a plot of the isoclines for equation (132). A phase trajectory, for a given set of initial conditions, is plotted by connecting short line segments with the proper slope at intervals along the isoclines. A trajectory with initial conditions $\theta(0) = 0$ and $V(0) = 0$ is plotted in figure 17.

Figure 17 shows the existence of singular points in the phase plane. A singular point is a representative point (θ_0, V_0) in the phase plane for which $(d\theta/dt) = (dV/dt) = 0$ (ref. 12). For a singular point, the direction of its tangent is indeterminate, and its trajectory degenerates into the singular point itself. From figure 17, the singular points

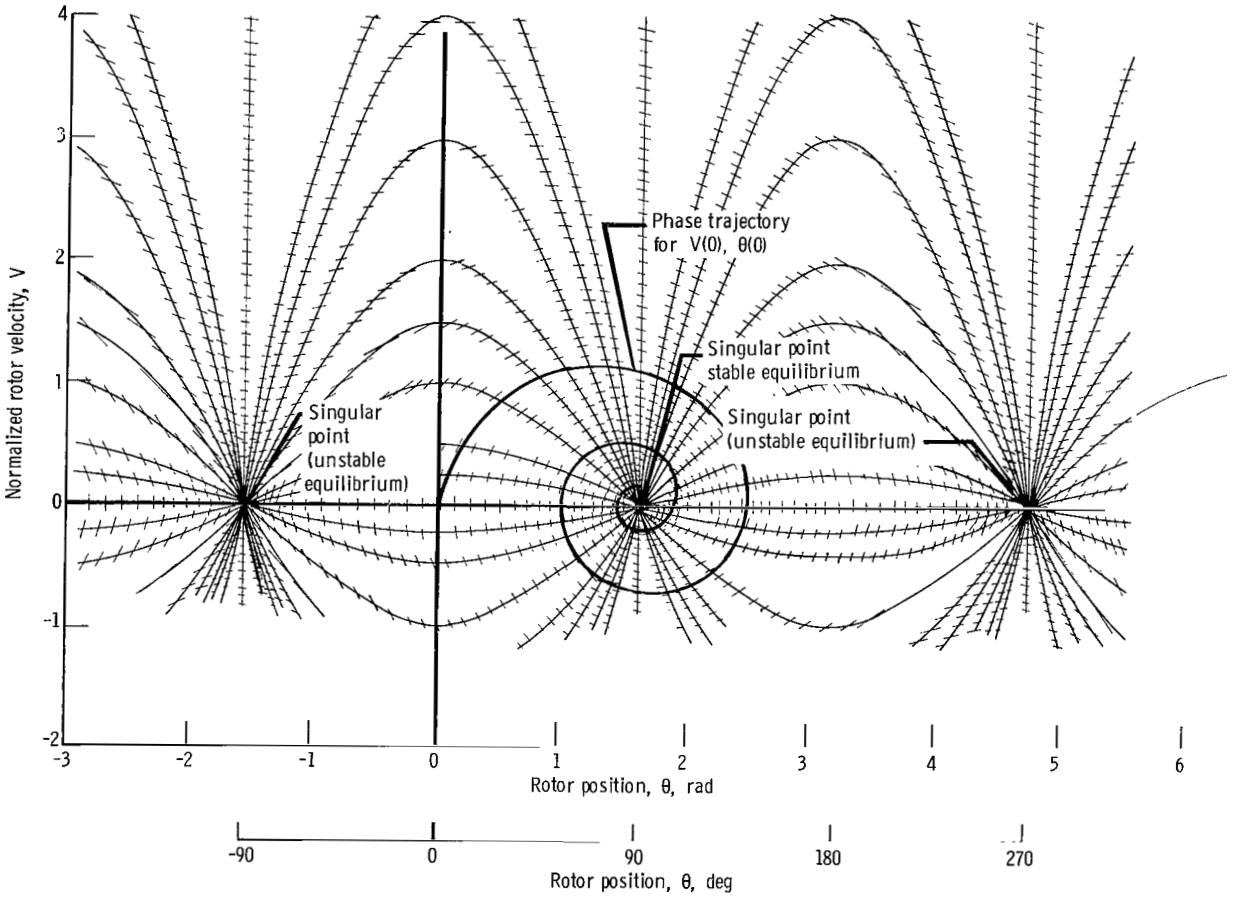

Figure 17. - Isoclines for $dV/d\theta = \cos \theta - 0.25$.

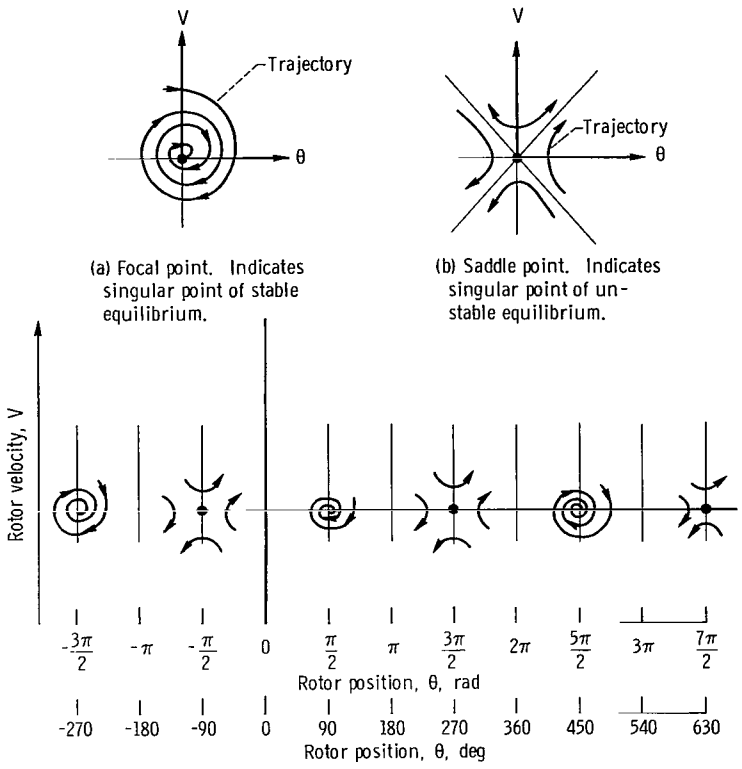

(a) Focal point. Indicates singular point of stable equilibrium.

(b) Saddle point. Indicates singular point of unstable equilibrium.

(c) Singular point locations for stepping motor equation.

Figure 18. - Types and locations of singular points for normalized stepping motor equation.

are found, for example, at $\theta = \pm 90^{\circ}$, $\pm 270^{\circ}$, and $\pm 450^{\circ}$. The singular points for these positions are either focal points or saddle points (ref. 13). Focal points are singularities in which trajectories approach in a decreasing spiral manner, as shown in figure 18(a). Focal points form points of stable equilibrium for the stepping motor. Saddle points are singularities which are approached by trajectories forming distinct sectioned curves, as shown in figure 18(b). Saddle points form points of unstable equilibrium. Figure 18(c) shows the alternating locations of focal points and saddle points. The focal points are 360° apart and 180° from the saddle points.

Multistep analysis. - Multistep operation can be analyzed for a given stepping sequence by plotting the isoclines of the resulting equations for the desired step commands. For a given stepping sequence, set of initial conditions, and stepping rate, the phase trajectory is developed by selecting the set of isoclines corresponding to the given step command. The phase trajectory is then drawn from the initial conditions. Time is computed incrementally along the trajectory. When the computed time equals the stepping period for the given command step, the next step command in the sequence is applied. The point on the trajectory at which the computed time equals the stepping period becomes the ini-

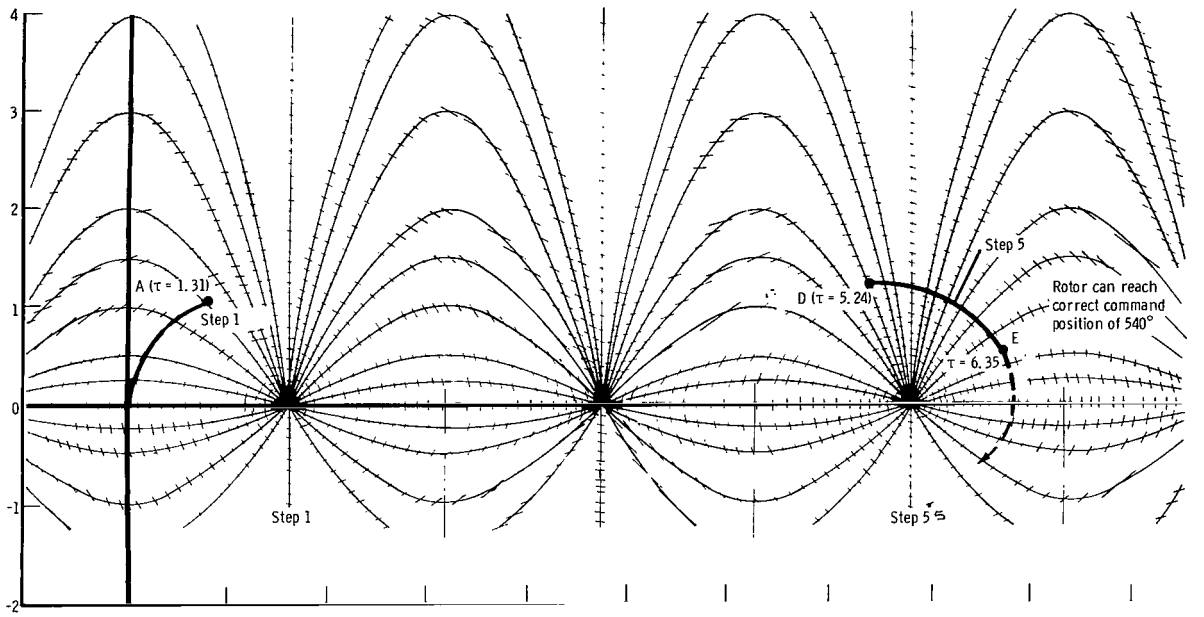

(a) Phase plane portrait for response to step commands 1 and 5. $dV/d\theta = \cos\theta/V - 0.25$.

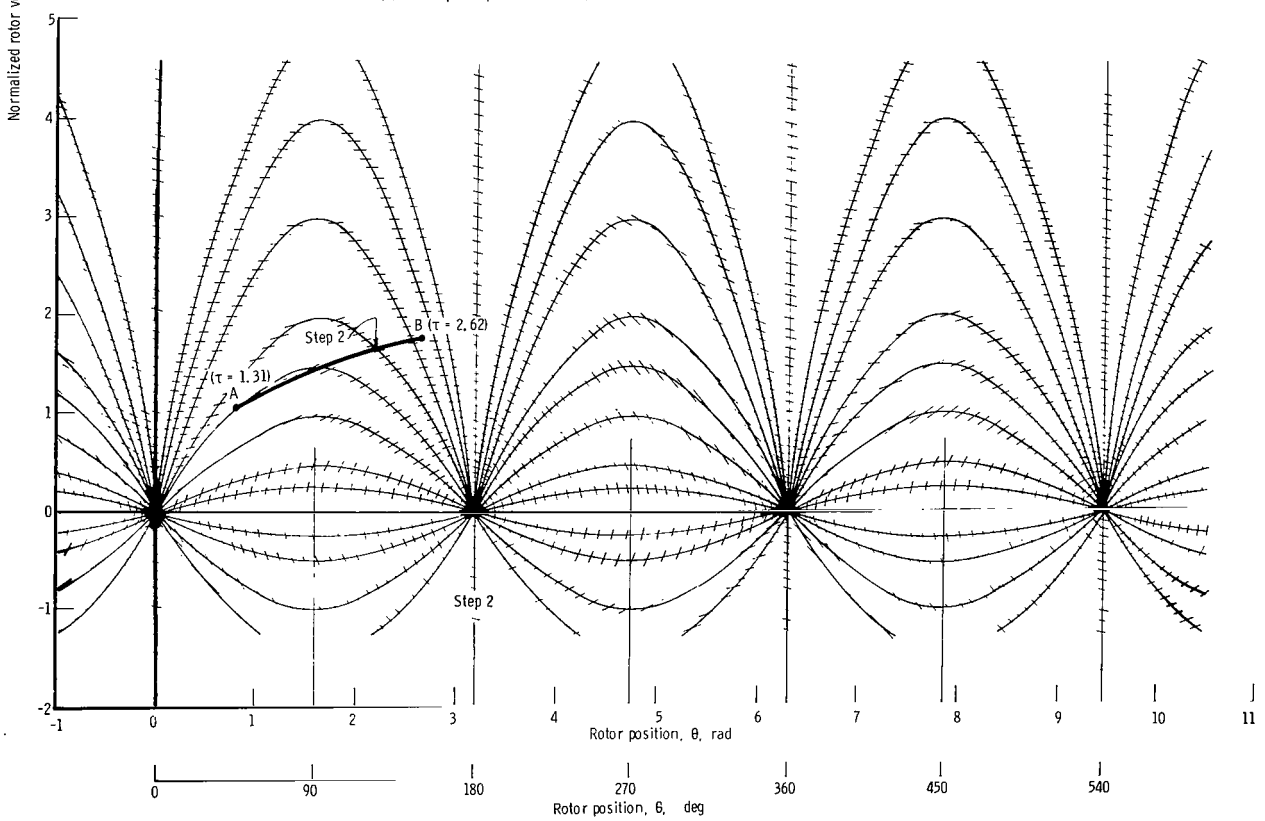

(b) Phase plane portrait for response to step command 2. $dV/d\theta = \sin\theta/V - 0.25$.

Figure 19. - Multistep sequence for change in normalized time $\Delta\tau$ of 1.31.

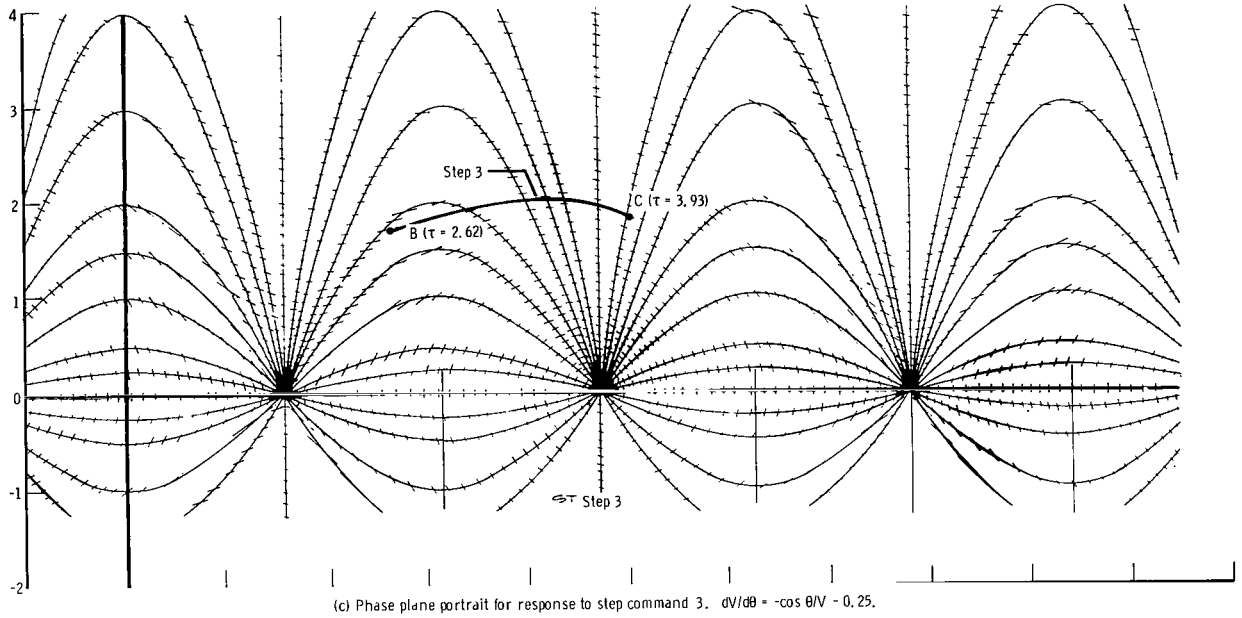

(c) Phase plane portrait for response to step command 3. $dV/d\theta = -\cos \theta/V - 0.25$.

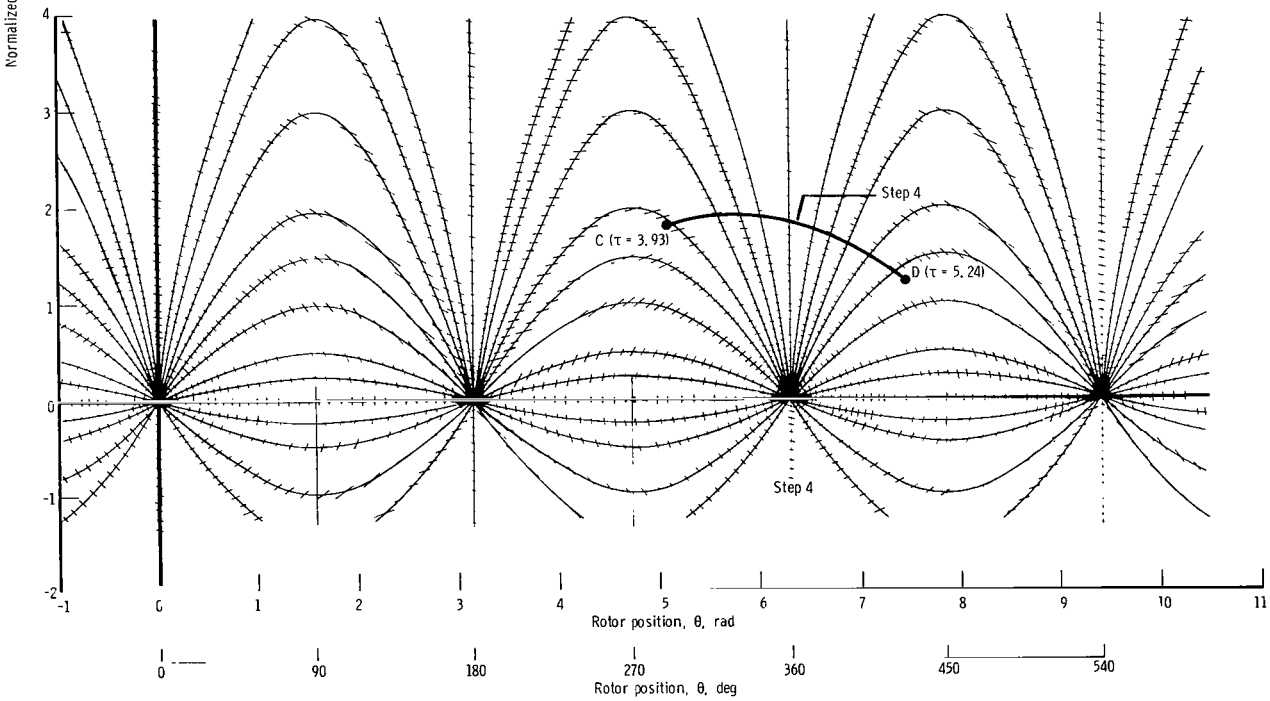

(d) Phase plane portrait for response to step command 4. $dV/d\theta = -\sin \theta/V - 0.25$.

Figure 19. - Concluded.

tial condition for the next step command. The trajectory for this step command is plotted by using its corresponding set of isoclines. Time is computed along the trajectory and compared with the stepping period to determine the application of the succeeding step command. This method is continued for the given stepping sequence.

Effect of stepping rate. - Figures 19(a) to (d) show the effect of stepping rate on the ability of the PM stepping motor to follow a set of sequential step commands. These figures show phase plane plots developed by the method of isoclines and consider the set of sequential step commands that were developed in equations (126) to (130). The equations for the slope of the trajectories with $\bar{D} = 0.25$ and $\bar{T}_L = 0$ are

Step 1: $$\theta_c = 90^o\left(\frac{\pi}{2} \text{ radians}\right); \frac{dV}{d\theta} = \frac{\cos\theta}{V} - 0.25 \tag{133}$$

Step 2: $$\theta_c = 180^o(\pi \text{ radians}); \frac{dV}{d\theta} = \frac{\sin\theta}{V} - 0.25 \tag{134}$$

Step 3: $$\theta_c = 270^o\left(\frac{3\pi}{2} \text{ radians}\right); \frac{dV}{d\theta} = -\frac{\cos\theta}{V} - 0.25 \tag{135}$$

Step 4: $$\theta_c = 360^o(2\pi \text{ radians}); \frac{dV}{d\theta} = -\frac{\sin\theta}{V} - 0.25 \tag{136}$$

Step 5: $$\theta_c = 450^o\left(\frac{5\pi}{2} \text{ radians}\right); \frac{dV}{d\theta} = \frac{\cos\theta}{V} - 0.25 \tag{137}$$

For the sequential step commands, again consider a normalized stepping period of $\Delta\tau = 1.31$. Recall that the step commands are applied at the following normalized times:

Step 1: $\tau = 0;\ \theta_c = 90^o\left(\frac{\pi}{2} \text{ radians}\right)$

Step 2: $\tau = 1.31;\ \theta_c = 180^o(\pi \text{ radians})$

Step 3: $\tau = 2.62;\ \theta_c = 270^o\left(\frac{3\pi}{2} \text{ radians}\right)$

Step 4: $\tau = 3.73;\ \theta_c = 360^o(2\pi \text{ radians})$

Step 5: $\tau = 5.24;\ \theta_c = 450^o\left(\frac{5\pi}{2} \text{ radians}\right)$

Step 1 calls for a position command of 90°. The trajectory for the response to this command is shown in figure 19(a). The rotor is assumed to be initially in equilibrium at $\theta(0) = 0$ and $V(0) = 0$. The trajectory is drawn from $\theta(0)$ and $V(0)$ to point A. At point A, the normalized time τ is 1.31, and the command for step 2 is applied. Step 2 calls for a position command of 180°. The trajectory for the response to this command is shown in figure 19(b) from point A to point B. At point B the computed time is 2.62, and the command for step 3 is applied. Step 3 calls for a position command of 270°. The trajectory for the response to this command is shown in figure 19(c) from point B to point C. At point C the computed time is 3.93, and the command for step 4 is applied. Step 4 calls for a position command of 360°. The trajectory for the response to this command is shown in figure 19(d) from point C to point D. At point D the computed time is 5.24, and the command for step 5 is applied. Step 5 calls for a position command of 450°. The slope of the trajectory in response to this command is given by equation (137). This equation gives the same result as for the slope of the trajectory in response to the 90° step command given by equation (133). Thus, the response for the 450° position command can be shown in figure 19(a) from point D to point E. This procedure can be continued for plotting the trajectory in response to any additional step commands desired.

Failure to execute commands. - Increasing the stepping rate decreases the amount of time in which the motor can respond to the step command. As a result, the rotor tends to lag behind the command position until sufficient velocity is built up to allow the rotor to reach the command position. The rotor can dynamically lag behind the command position by as much as 180° (two steps) and still follow the command. But once the rotor falls behind by more than 180°, the motor cannot reach the correct command position.

As an illustration, consider the previous step sequence with the normalized stepping period $\Delta\tau$ reduced from 1.31 to 0.92. The step commands are applied at the following times:

Step 1': $\tau = 0;\ \theta_c = 90^{\circ}\left(\frac{\pi}{2} \text{ radians}\right)$

Step 2': $\tau = 0.92;\ \theta_c = 180^{\circ}(\pi \text{ radians})$

Step 3': $\tau = 1.84;\ \theta_c = 270^{\circ}\left(\frac{3\pi}{2} \text{ radians}\right)$

Step 4': $\tau = 2.76;\ \theta_c = 360^{\circ}(2\pi \text{ radians})$

Step 5': $\tau = 3.68;\ \theta_c = 450^{\circ}\left(\frac{5\pi}{2} \text{ radians}\right)$

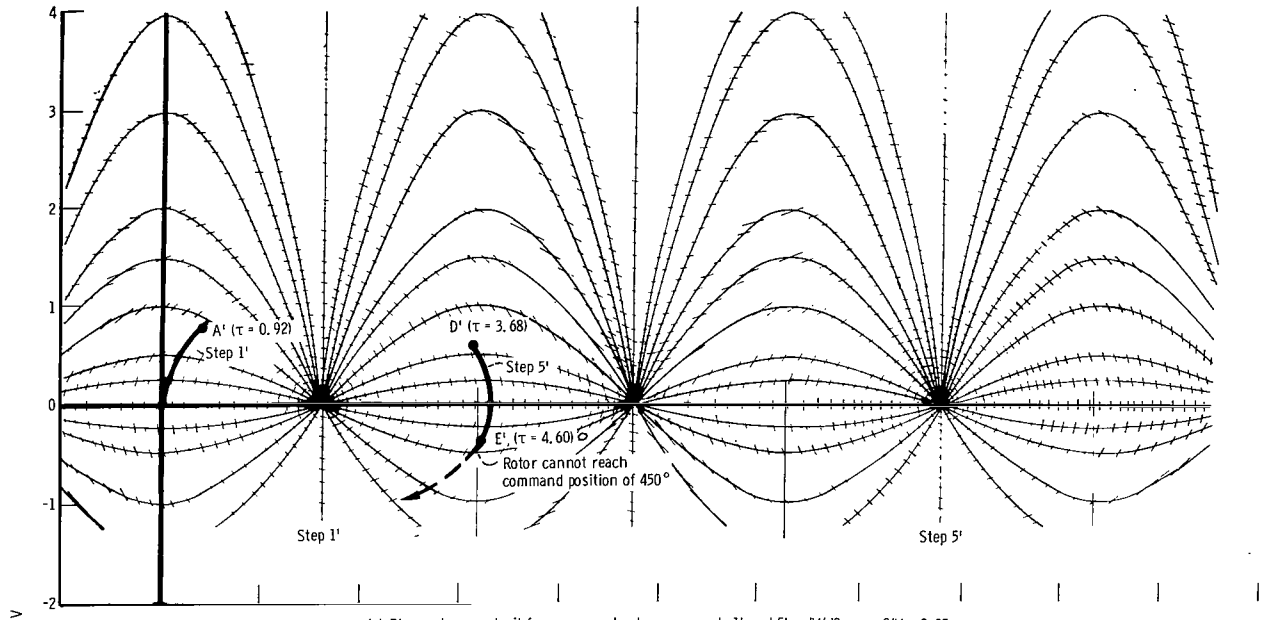

(a) Phase plane portrait for response to step commands 1' and 5'. $dV/d\theta = \cos\theta/V - 0.25$.

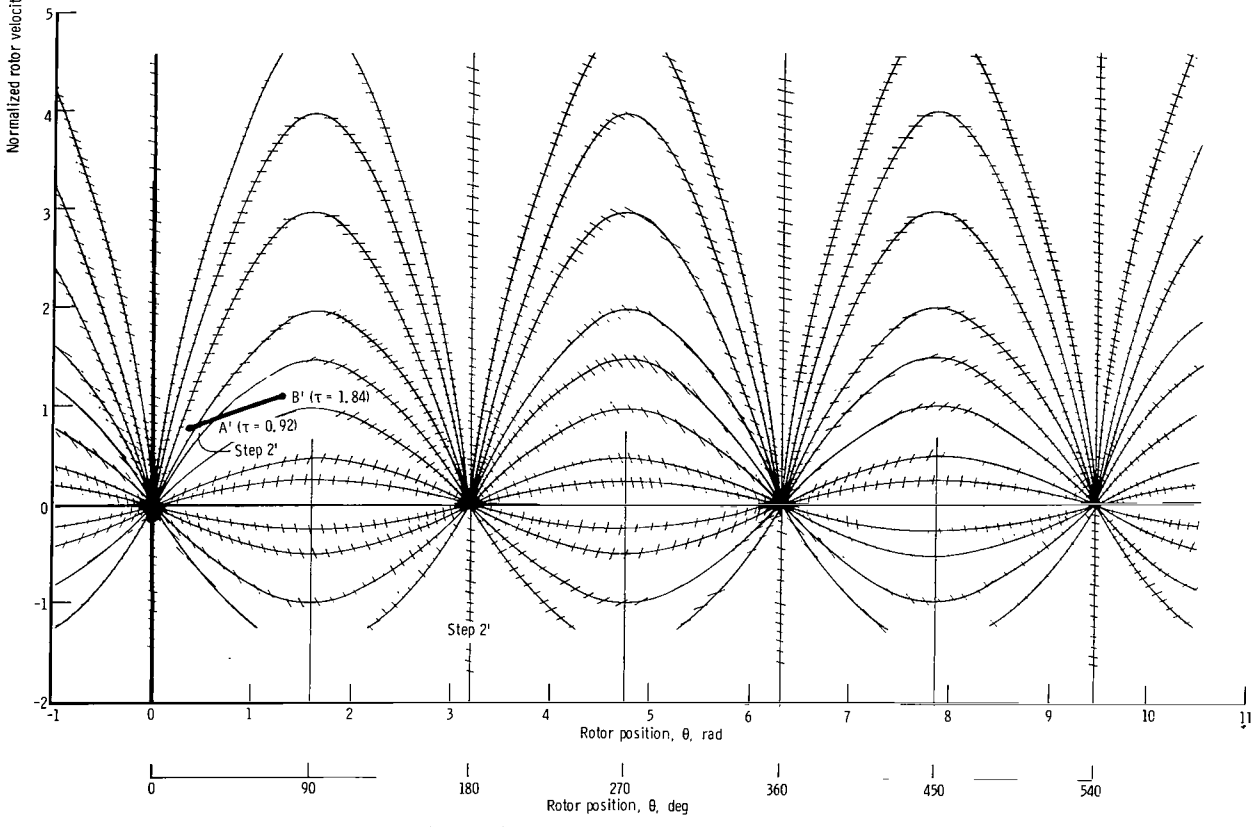

(b) Phase plane portrait for response to step command 2'. $dV/d\theta = \sin\theta/V - 0.25$.

Figure 20. - Multistep sequence for change in normalized time $\Delta\tau$ of 0.92.

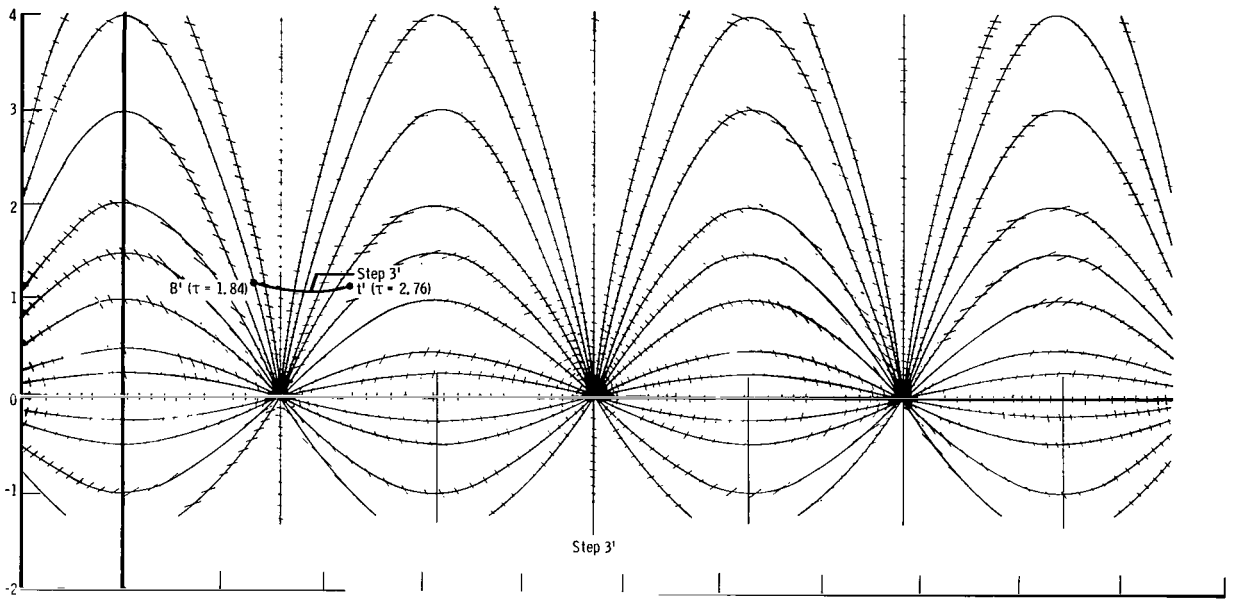

(c) Phase plane portrait for response to step command 3'. $dV/d\theta = -\cos \theta/V - 0.25$.

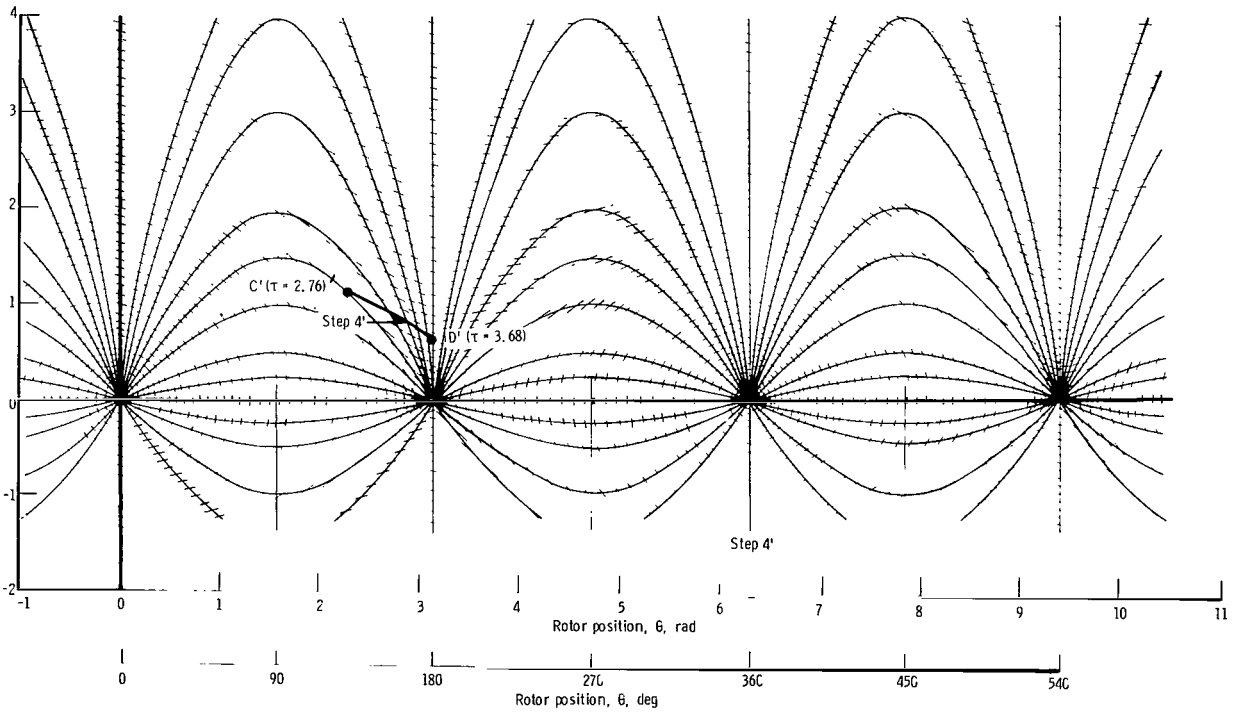

(d) Phase plane portrait for response to step command 4'. $dV/d\theta = -\sin \theta/V - 0.25$.

Figure 20. - Concluded.

The response to step 1' is shown in figure 20(a) from $V(0) = 0$ and $\theta(0)$ to point A'. At point A', $\tau = 0.92$, and the 180° step command is applied. Notice that the value of velocity and position reached is considerably lower than in the previous case for $\tau = 1.31$. Figure 20(b) shows the trajectory for the response to the 180° step command between points A' and B'. Note in figure 20(b) that the rotor position at point B' is lagging the command position by more than 90°. At point B', $\tau = 1.84$, and the step command for 270° is applied. Figure 20(c) shows the trajectory for the response to the 270° step command, between points B' and C'. The velocity of the rotor actually decreases during this step, and the rotor lags further behind the command position. At point C', $\tau = 2.76$, and the 360° step command is applied. Note by examining the isoclines, that had the 360° step command not been applied, the rotor could still have reached the correct command position of 270°. Figure 20(d) shows the trajectory for the response to the 360° step command between points C' and D'. Again during the step the rotor velocity decreases. At point D' the rotor is approximately 180° behind the command position. However, the rotor can still reach the proper command position of 360°. At point D', $\tau = 3.68$, and the 450° step command is applied. Figure 20(a) shows the response to the 450° step command between points D' and E'. The rotor is more than 180° behind the command position during the entire step. Clearly, the motor cannot reach the desired command position of 450°. If no further steps are applied, the rotor will come to rest at $\theta = 90^{\circ}$, or four steps behind the desired command position.

In general, the rotor will fail to execute the step command if the stepping motor trajectory crosses the position axis before the desired command position is reached. This can only occur if the position of the rotor lags the step command by more than 180°. The failure analysis must be carried out by using enough steps to show that either the motor fails to follow the desired command or that the motor reaches a steady-state condition for the given command rate.

If a motor will follow step commands at a given stepping rate, it will follow the step commands regardless of the number of steps applied. Also, if it cannot follow a step command, the motor will continue to lose steps. The steps that it loses can be applied after the step commands have been completed. This can be accomplished by feedback but introduces more complications (ref. 1).

The method of isoclines is not limited to analyzing step commands in one direction or to a constant time between steps. Any step sequence or stepping rate can be considered by selecting the proper set of isoclines corresponding to the step sequence. In general any step sequence or stepping rate can be considered by selecting the proper set of isoclines corresponding to the step sequence. Thus, any input step sequence can be investigated by this method.

DIMENSIONLESS CURVES FOR EXPRESSING PM STEPPING MOTOR PERFORMANCE

Multistep operation in the phase plane has been shown to be a function of three dimensionless parameters:

(1) Motor damping parameter, $\overline{D} = 2\zeta$ (138)

(2) Time parameter, $\tau = \sqrt{\frac{N_{RT}\sqrt{2}\,K_T I}{J}}\,t = \omega_N t$ (139)

(3) Load torque parameter, $T_L = \frac{T_L}{\sqrt{2}\,K_T I} = \frac{T_L}{T_S}$ (140)

Using these parameters, multistep analysis in the phase plane can be used to specify the maximum stepping rate for any given PM stepping motor and desired value of load torque.

The maximum stepping rate is defined as the rate in which the motor can step with a given value of load torque and not miss a single step. The PM stepping motor is assumed to be initially at rest at a point of stable equilibrium for the given value of load torque. By determining the maximum stepping rate for various values of $\overline{D}$ and $\overline{T}_L$, a set of dimensionless curves can be developed to predict PM stepping motor performance.

A computer program was developed which uses the delta method to map the maximum stepping rate as a function of $\overline{D}$ and $\overline{T}_L$ and is described in appendix C. In the computer program, the maximum stepping rate is determined by an iteration process. A normalized stepping rate $1/\Delta\tau$ is chosen and expressed in terms of the time between application of steps $\Delta\tau$. The motor is then stepped at the given rate for a number of steps. The phase portrait is examined to see if the motor follows the command without missing a step. If the motor follows the command, a higher stepping rate is chosen, and the procedure is repeated until a stepping rate is found in which the motor cannot follow.

Figure 21 shows the resulting dimensionless curves of PM stepping motor performance derived from the computer program. The curves show that, for a given value of load torque, the maximum stepping rate of a given PM stepping motor decreases as the damping ratio increases. This has a direct bearing on the application of the PM stepping motor to system design. The motion of the PM stepping motor for a single step is highly underdamped, yielding low values of damping ratio. The motor can be compensated to obtain a higher damping ratio and a better single-step response. But raising the value of

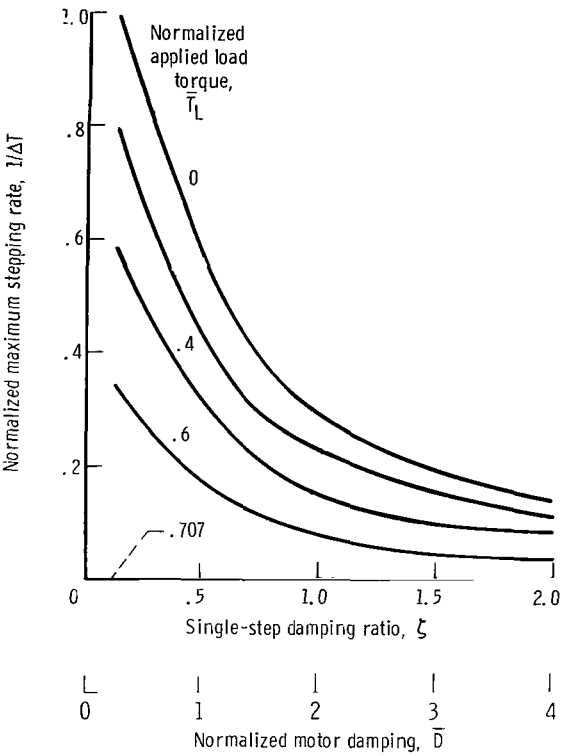

Figure 21. - Dimensionless parameter curves for permanent magnet stepping motor.

the damping ratio decreases the maximum stepping rate that can be obtained. Thus, for multistep operation, compensating for the single-step response may not be desirable.

The phase plane analysis demonstrated that the ability of a motor to follow a set of step commands was, in part, determined by the position of the rotor corresponding to the command position during each succeeding step. If the rotor position falls further behind with each succeeding step, the motor will eventually miss a step. Thus, the rise time and, hence, the damping ratio of the rotor during each step affects the maximum stepping rate of the PM stepping motor. The damping ratio is given by

$$\zeta = \frac{D}{2J\omega_N} \tag{141}$$

Thus, the damping ratio can be lowered by decreasing the viscous damping or increasing the motor inertia or the natural frequency. However, increasing the inertia decreases the natural frequency since

$$\omega_N = \frac{\tau}{t} = \sqrt{\frac{N_{RT}\sqrt{2}\,K_T I}{J}} \tag{142}$$

If the natural frequency of the motor is increased, the time between steps can be decreased, and the maximum stepping rate can be increased since

$$\Delta\tau = \omega_N \Delta t \tag{143}$$

$$\frac{1}{\Delta t} = \frac{\omega_N}{\Delta\tau} \tag{144}$$

Thus, for a given load torque, maximum stepping rate is obtained by minimizing the damping ratio and maximizing the natural frequency.

Figure 21 also shows that, for a given damping ratio, increasing the load torque decreases the maximum stepping rate that can be achieved. Since the dimensionless curves assume a constant current source, the maximum stepping rate will be decreased if the motor is driven from a voltage source. The stepping rate in this case is decreased as a result of the stator winding L/R time constant and induced emf, both of which cause the rotor position to further lag behind the intended command position.

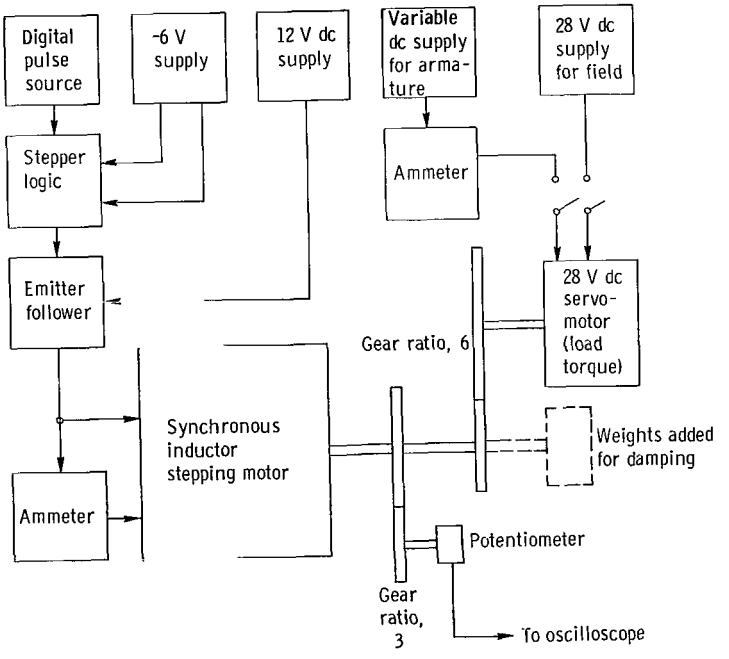

Figure 22.- Experimental setup for verification of analytical model.

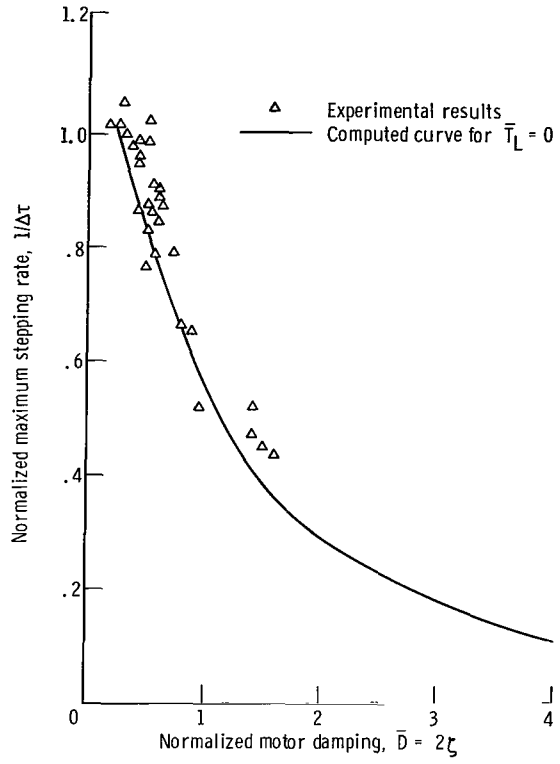

Figure 23. - Experimental verification of dimensionless parameter curves for normalized applied load torque $\bar{T}_L$ of 0.

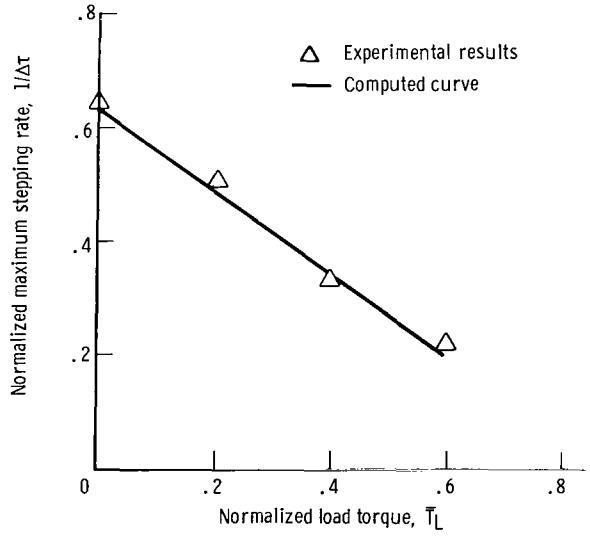

Figure 24. - Experimental verification of normalized stepping rate for various values of load torque with normalized damping $\bar{D}$ of 0.9.

EXPERIMENTAL VERIFICATION OF DIMENSIONLESS CURVES

Some experimental measurements were taken to check the validity of the dimensionless curves developed for the PM stepping motor. Figure 22 is a schematic diagram of the apparatus used in the experimental work. The measurements were taken on synchronous inductor stepping motors. The stepping motor drive circuit used approximated a current source. Damping torque was obtained by adding weights to the motor's output shaft. Additional damping torque was obtained by coupling to the stepping motor output shaft a dc servomotor whose field windings were open-circuited. Load torque was obtained by using the servomotor in the conventional manner.

Figure 23 shows a comparison of the experimental values obtained to the analytically derived curve for $\overline{T}_L = 0$. The experimental data show reasonable agreement with the analytical curve.

Figure 24 shows the comparison of experimental data with the corresponding analytical data from the dimensionless curves for values of $\overline{T}_L$ of 0, 0.2, 0.4, and 0.6. The normalized damping was held at 0.9. The results show good agreement.

CONCLUSIONS

An analysis of the permanent magnet (PM) stepping motor can be used to study the effects of inertia, damping, current transients, etc., on the stepping motor response to a single-step command. A nonlinear analysis which uses phase plane techniques was developed. This analysis allows the PM stepping motor to be analyzed for failure to respond to given stepping rates with various values of load and friction. The nonlinear analysis was simplified by assuming that the stator windings are supplied by a constant current drive circuit that could compensate for the electrical (L/R) time constant. Thus, the results represent an upper bound on stepping motor performance.

Based on the nonlinear analysis, it was found that the PM stepping motor cannot respond to a step command when the applied load torque becomes greater than 0.707 of the motor's stall torque. The PM stepping motor cannot follow a sequential set of step commands if, during the sequence, the rotor lags the command position by more than two steps.

This result was extended to develop a set of dimensionless curves which express maximum normalized stepping rate as a function of normalized damping and normalized applied load torque. These curves allow the maximum stepping rate of a permanent magnet stepping motor to be determined from simple measurements of its parameters or from manufacturer's data.

Because the dimensionless curves assume a constant current source, the maximum stepping rate will be decreased if the motor is driven from a voltage source. The stepping rate in this case will be decreased as a result of the stator winding electrical (L/R) time constant and induced electromotive force, both of which cause the rotor position to further lag behind the intended command position.

Stepping motor response to a single-step command is usually highly underdamped. However, the maximum stepping rate curves show that improving the single-step response by adding damping will lower the maximum stepping rate that can be achieved.

Lewis Research Center,
National Aeronautics and Space Administration,
Cleveland, Ohio, November 19, 1968,
122-29-03-01-22.

APPENDIX A

SYMBOLS

B	magnetic flux density, T
D	viscous damping of motor and load, $(g)(cm^2)/sec$
$\overline{D}$	normalized damping
E	constant value of stator input voltage, V
E(S)	Laplace transform of $\rho(t)$, V
E(t)	stator input voltage, V
E_v	stator induced electromotive force (emf), V
I	constant value of stator input current, A
I(S)	Laplace transform of $l(t)$
I(t)	stator input current, A
J	inertia of motor and load, $(g)(cm^2)$
K_I	solenoid constant, $(\Omega)(sec)/m^2$
K_m	bar magnet constant, $m/(\Omega)(sec)$
K_T	motor torque constant, (N-m)/A
K_v	constant relating induced voltage and stator flux density, (V)(sec)/deg
L	stator inductance per phase, H
$\mathscr{L}[\ ]$	Laplace transformation
l	length of bar magnet, cm
M	magnetic moment, $(A)(m^2)$
m	bar magnet pole strength, Wb
N_{RT}	constant relating rotor position in degrees θ to mechanical degrees of rotation
n	number of solenoid turns
R	stator resistance per phase, Ω
S	Laplace operator, 1/sec
T_D	developed motor torque, N-m
$T_f(t)$	frictional torque, N-m
$\overline{T}_f$	normalized frictional torque
$T_L(t)$	applied load torque, N-m
$\overline{T}_L$	normalized applied load torque
T_{max}	maximum motor torque per phase, N-m
T_S	motor stall torque, both phases energized, N-m
t	time, sec
V	normalized velocity
X(t)	variable
α	angular measurement variable, deg
β	line segment, cm
$\Delta(\ )$	change in a variable about an operating point
δ	center of circular arc, deg
ζ	damping ratio
$\theta(S)$	Laplace transform of $\theta(t)$, specified in degrees except where noted in radians

$\theta(t)$	rotor position defined so that 1/4 rotor tooth pitch equals 90^{o}, specified in degrees except where noted in radians
θ_c	rotor command position, specified in degrees except where noted in radians
τ	normalized time
$\Delta\tau$	change in normalized time
$1/\Delta\tau$	normalized stepping rate
$\varphi(t)$	rotor position in mechanical degrees
ω_N	natural frequency, rad/sec
(0)	initial condition of a variable

Subscripts:

0	value at operating point
1	stator phase 1
2	stator phase 2

APPENDIX B

LAPLACE TRANSFORM DERIVATIONS OF LINEARIZED FUNCTIONS

The Laplace transformation can be applied by considering the following development. For a variable X(t) about an operating point,

$$X(t) = X_0 + \Delta X(t) \tag{B1}$$

$$\frac{dX(t)}{dt} = \left(\frac{dX}{dt}\right)_0 + \Delta\left[\frac{dX(t)}{dt}\right] \tag{B2}$$

$$\frac{d^2X(t)}{dt^2} = \left(\frac{d^2X}{dt^2}\right)_0 + \Delta\left[\frac{d^2X(t)}{dt^2}\right] \tag{B3}$$

and so forth. Taking the derivative of equation (B1) and assuming that X_0 is a constant,

$$\frac{d}{dt}X(t) = \frac{d}{dt}(X_0) + \frac{d}{dt}\Delta X(t) \tag{B4}$$

Combining equations (B2) and (B4),

$$\Delta\left[\frac{dX(t)}{dt}\right] = \frac{d}{dt}\Delta X(t) - \left(\frac{dX}{dt}\right)_0 \tag{B5}$$

Taking the Laplace transform of equation (B5),

$$\mathscr{L}\left\{\Delta\left[\frac{dX(t)}{dt}\right]\right\} = S\mathscr{L}\left[\Delta X(t)\right] - \Delta X(0) - \frac{\left(\frac{dX}{dt}\right)_0}{S} \tag{B6}$$

In the same manner, taking the derivative of equation (B2),

$$\frac{d}{dt}\left[\frac{d}{dt}X(t)\right] = \frac{d}{dt}\left(\frac{dX}{dt}\right)_0 + \frac{d}{dt}\left\{\Delta\left[\frac{dX(t)}{dt}\right]\right\} \tag{B7}$$

Combining equations (B3) and (B7) results in

$$\Delta\left[\frac{d^2X(t)}{dt^2}\right] = \frac{d}{dt}\left\{\Delta\left[\frac{dX(t)}{dt}\right]\right\} - \left(\frac{d^2X}{dt^2}\right)_0 \tag{B8}$$

Taking the Laplace transformation of equation (B8),

$$\mathcal{L}\left\{\Delta\left[\frac{d^2X(t)}{dt^2}\right]\right\} = S\mathcal{L}\left\{\Delta\left[\frac{dX(t)}{dt}\right]\right\} - \Delta\left[\frac{dX(0)}{dt}\right] - \frac{\left(\frac{d^2X}{dt^2}\right)_0}{S}$$

$$= S^2\mathcal{L}\left[\Delta X(t)\right] - S\,\Delta X(0) - \left(\frac{dX}{dt}\right)_0 - \Delta\left[\frac{dX(0)}{dt}\right] - \frac{\left(\frac{d^2X}{dt^2}\right)_0}{S} \tag{B9}$$

When the initial conditions are used, the Laplace transforms of the excursions about the operating point at the beginning of the step are

$$\mathcal{L}\left[\Delta\theta(t)\right] = \Delta\theta(S) \tag{B10}$$

$$\mathcal{L}\left\{\Delta\left[\frac{d\theta(t)}{dt}\right]\right\} = S\,\Delta\theta(S) - \Delta\theta(0) - \frac{\left(\frac{d\theta}{dt}\right)_0}{S} = S\,\Delta\theta(S) \tag{B11}$$

$$\mathcal{L}\left\{\Delta\left[\frac{d^2\theta(t)}{dt^2}\right]\right\} = S^2\,\Delta\theta(S) - S\,\Delta\theta(0) - \left(\frac{d\theta}{dt}\right)_0 - \Delta\left[\frac{d\theta(0)}{dt}\right] - \frac{\left(\frac{d^2\theta}{dt^2}\right)_0}{S} = S^2\,\Delta\theta(S) \tag{B12}$$

$$\mathcal{L}\left[\Delta E_2(t)\right] = \Delta E_2(S) \tag{B13}$$

$$\mathcal{L}\left[\Delta I_2(t)\right] = \Delta I_2(S) \tag{B14}$$

$$\mathscr{L}\left\{\Delta\left[\frac{dI_2(t)}{dt}\right]\right\} = S\,\Delta I_2(S) - \Delta I_2(0) - \frac{\left(\frac{dI_2}{dt}\right)_0}{S} = S\,\Delta I_2(S) - \frac{\left(\frac{dI_2}{dt}\right)_0}{S} \tag{B15}$$

$$\mathscr{L}\left[\Delta I_1(t)\right] = \Delta I_1(S) \tag{B16}$$

$$\mathscr{L}\left\{\Delta\left[\frac{dI_1(t)}{dt}\right]\right\} = S\,\Delta I_1(S) - \Delta I_1(0) - \frac{\left(\frac{dI_1}{dt}\right)_0}{S} = S\,\Delta I_1(S) \tag{B17}$$

The derivative $(dI_2/dt)_0$ in equation (B15) can be determined by noting that since $(d\theta/dt)_0 = 0$, the induced voltage $E_{v,0} = 0$. The voltage supplied to winding 2 becomes

$$\Delta E_2(t) = \Delta I_2(t)R + \Delta\left[\frac{dI_2(t)}{dt}\right]L \tag{B18}$$

$$\Delta E_2(S) = (R + LS)\Delta I_2(S) \tag{B19}$$

Assuming that the stator input voltage to winding 2 is a step function results in

$$I_2(S) = \frac{E_{2,0}}{S}\left(\frac{1}{R + LS}\right) \tag{B20}$$

or

$$\mathscr{L}\left[\frac{dI_2(t)}{dt}\right] = SI_2(S) = \frac{E_{2,0}}{R + LS} \tag{B21}$$

When the initial value theorem (ref. 14) is applied,

$$\lim_{t\to 0} \frac{dI_2(t)}{dt} = \lim_{S\to\infty} \frac{SE_{2,0}}{R + LS} = \frac{E_{2,0}}{L} = \left(\frac{dI_2}{dt}\right)_0 \tag{B22}$$

Thus, the Laplace transforms of the equations for the excursions about the operating point at the beginning of the step become

$$\left(\frac{JS^2}{N_{RT}} + \frac{DS}{N_{RT}} + \sqrt{K_T^2 I_{1,0}^2 - T_{L,0}^2}\right)\Delta\theta(S) = K_T \sqrt{1 - \frac{T_{L,0}^2}{K_T^2 I_{1,0}^2}}\ \Delta I_2(S)$$

$$+ \frac{T_{L,0}}{I_{1,0}}\Delta I_1(S) - \Delta T_L(S) \qquad \text{(B23)}$$

$$\Delta I_2(S) = \frac{\Delta E_2(S) + \dfrac{E_{2,0}}{S} - \dfrac{K_V}{N_{RT}}\sqrt{1 - \dfrac{T_{L,0}^2}{K_T^2 I_{1,0}^2}}\ S\,\Delta\theta(S)}{R + LS} \qquad \text{(B24)}$$

$$\Delta I_1(S) = \frac{\dfrac{K_V T_{L,0}}{N_{RT} K_T I_{1,0}}\ S\,\Delta\theta(S)}{R + LS} \qquad \text{(B25)}$$

Combining equations (B22) to (B24) gives the resultant linearized transfer function about an operating point at the beginning of a step:

$$\Delta\theta(S) = \frac{K_T \sqrt{1 - \dfrac{T_{L,0}^2}{K_T^2 I_{1,0}^2}}\left[\Delta E_2(S) + \dfrac{E_{2,0}}{S}\right] - (R + LS)\Delta T_L(S)}{\dfrac{JLS^3}{N_{RT}} + \left(\dfrac{DL + JR}{N_{RT}}\right)S^2 + \left(\dfrac{DR}{N_{RT}} + \dfrac{K_T K_V}{N_{RT}} + LK_T I_{1,0}\sqrt{1 - \dfrac{T_{L,0}^2}{K_T^2 I_{1,0}^2}}\right)S + RK_T I_{1,0}\sqrt{1 - \dfrac{T_{L,0}^2}{K_T^2 I_{1,0}^2}}}$$

(B26)

APPENDIX C

DIMENSIONLESS PARAMETER CURVE COMPUTER PROGRAM

A digital computer program was written to develop the dimensionless curves using the multistep phase plane analysis. The maximum stepping rate was determined by stepping the motor a number of steps at a constant stepping rate. The phase trajectory was calculated and checked to see if it followed the command without missing a step. The stepping rate was increased until the motor failed to follow a command.

The computer program developed is shown in table I. The program was developed by using the delta method for computing the phase trajectories. The delta method allowed the trajectory to be calculated by using small incremental sections. This method was also convenient for calculating time along the trajectory. The computer input variables were

(1) Initial velocity, VIN

(2) Initial position, THIN

(3) Initial value of δ, DELTIN

(4) Total time for the number of steps, TTOT

(5) Total time between steps, DTAUS

(6) Position increment used in computing trajectory, DTH

(7) Normalized motor damping parameter, D

(8) Normalized load torque, TL

Twenty steps were commanded for each stepping rate. These were enough steps to determine whether the motor could follow the stepping rate with the given $\overline{D}$ and $\overline{T}_L$. Motor failure was determined by checking for the rotor velocity to change sign (motor reverses its direction) before the desired step command was reached. The stepping rates were varied in increments of 0.01, and the values of position were compared along the trajectory. The normalized time was computed, and a new value for delta was computed for each time the position of the rotor changed by a predetermined increment. This increment affects the overall accuracy of the trajectory and of the calculated time. Thus, it was made an input variable (DTH), and its effect on the response was checked. A value of DTH = 0.05 was found to give results with sufficient accuracy for the program.

The maximum stepping rate was computed, using this program, for values of D = 0.25, 0.5, 1.0, 1.5, 2.0, and 4.0 and for values of $\overline{T}_L$ = 0, 0.2, 0.4, and 0.6.

TABLE I. - DIGITAL COMPUTER PROGRAM

```
100 FORMAT(8E10.5)
101 FORMAT(1H1,5X,3HVIN,9X,4HTHIN,7X,6HDELTIN,9X,4HTTOT,8X,5HDTAUS,
    10X1,3HDTH,11X,1HD,11X,2HTL/(8E13.5))
102 FORMAT(3E20.6)
103 FORMAT(1HO,5X,8HVELOCITY,14X,5HTHETA,15X,3HTAU)
500 READ(5,100)VIN,THIN,DELTIN,TTOT,DTAUS,DTH,D,TL
    WRITE(6,101)VIN,THIN,DELTIN,TTOT,DTAUS,DTH,D,TL
    WRITE(6,103)
    TAU=0.0
    SIGN=1.0
    V1=VIN
    TH1=THIN
    WRITE(6,102)V1,TH1,TAU
    DELTA=DELTIN
    N=1
    M=1
 10 RADSQ=(V1*V1+(DELTA+TH1)*(DELTA+TH1))
    TH2=TH1+DTH
    TEM1=(DELTA+TH2)*(DELTA+TH2)
    IF(TEM1.LE.RADSQ) GO TO 20
    TH2=TH2-DTH
    DTH=-DTH
    SIGN=-SIGN
    TEM1=(DELTA+TH2)*(DELTA+TH2)
 20 V2=SIGN*SQRT(RADSQ-TEM1)
    IF(TEM1.GT.RADSQ) GO TO 21
    DTAU=2.0*(TH2-TH1)/(V2+V1)
 21 TAU=TAU+DTAU
    V1=V2
    TH1=TH2
    K=M-(M/5)*5
    IF(K)60,60,70
 60 WRITE(6,102)V1,TH1,TAU
 70 M=M+1
    IF(TAU.GT.TTOT) GO TO 500
 30 TEM=TAU-FLOAT(N-1)*DTAUS*4.0
    TEM2=TEM/DTAUS
    IF(TEM2.GT.4.0) GO TO 40
    GO TO 50
 40 N=N+1
    GO TO 30
 50 IF(TEM2.GT.3.0) GO TO 14
    IF(TEM2.GT.2.0) GO TO 13
    IF(TEM2.GT.1.0) GO TO 12
 11 VDV=COS(TH1)-D*V1-TL
    GO TO 15
 12 VDV=SIN(TH1)-D*V1-TL
    GO TO 15
 13 VDV=-COS(TH1)-D*V1-TL
    GO TO 15
 14 VDV=-SIN(TH1)-D*V1-TL
 15 DELTA=-VDV-TH1
    GO TO 10
    END
```

REFERENCES

1. Proctor, John: Stepping Motors Move In. Product Eng., vol. 34, Feb. 4, 1963, pp. 74-78.

2. Nicklas, J. C.: Analysis, Design and Testing of a Position Servo Utilizing a Stepper Motor. Tech. Rep. 32-206, Jet Propulsion Lab., California Inst. Tech., Jan. 25, 1962.

3. Giles, S.; and Marcus, A. A.: SNAP-8-Control-Drum Actuators. Rep. NAA-SR-9645, Atomics International, Dec. 15, 1964.

4. Bailey, S. J.: Incremental Servos. Part I - Stepping vs Stepless Control. Control Eng., vol. 7, no. 11, Nov. 1960, pp. 123-127; Part II - Operation and Analysis, vol. 7, no. 12, Dec. 1960, pp. 97-102; Part III - How They've Been Used, vol. 8, no. 1, Jan. 1961, pp. 85-88; Part IV - Today's Hardware, vol. 8, no. 3, Mar. 1961, pp. 133-135; Part V - Interlocking Steppers, vol. 8, no. 5, May 1961, pp. 116-119.

5. O'Donohue, John P.: Transfer Function for a Stepper Motor. Control Eng., vol. 8, no. 11, Nov. 1961, pp. 103-104.

6. Kieburtz, R. Bruce: The Step Motor - The Next Advance in Control Systems. IEEE Trans. on Automatic Control, vol. AC-9, no. 1, Jan. 1964, pp. 98-104.

7. Snowdon, Arthur E.; and Madsen, Elmer W.: Characteristics of a Synchronous Inductor Motor. AIEE Trans. on Applications and Industry, vol. 81, Mar. 1962, pp. 1-5.

8. Morgan, N. L.: Versatile Inductor Motor Used in Solving Industrial Control Problems. Plant Eng., vol. 16, no. 6, June 1962, pp. 143-146.

9. Swonger, C. W.: Polyphase Motors as Digital-Analog Stepping Devices. Data Systems Eng., vol. 18, no. 6, July-Aug. 1963, pp. 52-56.

10. Graham, Dunstan; and McFuer, Duane: Analysis of Nonlinear Control Systems. John Wiley & Sons, Inc., 1961.

11. Zeller, Donald F.: Digital Control of a Stepping Motor. MS Thesis, Massachusetts Inst. Tech., 1966.

12. Cunningham, W. J.: Introduction to Nonlinear Analysis. McGraw-Hill Book Co., Inc., 1958.

13. Minorsky, Nicholas: Introduction to Non-Linear Mechanics. J. W. Edwards, Ann Arbor, 1947.

14. Savant, C. J., Jr.: Basic Feedback Control System Design. McGraw-Hill Book Co., Inc., 1958, p. 64.

NATIONAL AERONAUTICS AND SPACE ADMINISTRATION
WASHINGTON, D.C. 20546

OFFICIAL BUSINESS

FIRST CLASS MAIL

POSTAGE AND FEES PAID
NATIONAL AERONAUTICS AND
SPACE ADMINISTRATION

02U 001 2M 51 3DS 69058 00903
AIR FORCE WEAPONS LABORATORY/AFWL/
KIRTLAND AIR FORCE BASE, NEW MEXICO 87117

ATT: [illegible], ACTING CHIEF TECH. LIB

POSTMASTER: If Undeliverable (Section 158 Postal Manual) Do Not Return

"The aeronautical and space activities of the United States shall be conducted so as to contribute . . . to the expansion of human knowledge of phenomena in the atmosphere and space. The Administration shall provide for the widest practicable and appropriate dissemination of information concerning its activities and the results thereof."

—NATIONAL AERONAUTICS AND SPACE ACT OF 1958

NASA SCIENTIFIC AND TECHNICAL PUBLICATIONS

TECHNICAL REPORTS: Scientific and technical information considered important, complete, and a lasting contribution to existing knowledge.

TECHNICAL NOTES: Information less broad in scope but nevertheless of importance as a contribution to existing knowledge.

TECHNICAL MEMORANDUMS: Information receiving limited distribution because of preliminary data, security classification, or other reasons.

CONTRACTOR REPORTS: Scientific and technical information generated under a NASA contract or grant and considered an important contribution to existing knowledge.

TECHNICAL TRANSLATIONS: Information published in a foreign language considered to merit NASA distribution in English.

SPECIAL PUBLICATIONS: Information derived from or of value to NASA activities. Publications include conference proceedings, monographs, data compilations, handbooks, sourcebooks, and special bibliographies.

TECHNOLOGY UTILIZATION PUBLICATIONS: Information on technology used by NASA that may be of particular interest in commercial and other non-aerospace applications. Publications include Tech Briefs, Technology Utilization Reports and Notes, and Technology Surveys.

Details on the availability of these publications may be obtained from:

SCIENTIFIC AND TECHNICAL INFORMATION DIVISION

NATIONAL AERONAUTICS AND SPACE ADMINISTRATION

Washington, D.C. 20546